University of Stavanger

FACULTY OF SCIENCE AND TECHNOLOGY

MASTER'S THESIS

Study programme/specialisation: MSc-Mathematics and Physics	Spring / Autumn semester, 20..21 Open / Confidential
Author: Karanvir Singh	
Programme coordinator: Stine Thu Johannessen Supervisor(s): Alex B. Nielsen	
Title of master's thesis: Quasi-Local Approaches to Black Hole Horizons and Rindler Trajectories in Dynamical Black Hole Spacetimes	
Credits: 60	
Keywords: Black hole Quasi-local Horizons General Relativity Gravity Rindler	Number of pages: 66 + supplemental material/other: …… Stavanger, 29/06/2021 date/year

Quasi-Local Approaches to Black Hole Horizons and Rindler Trajectories in Dynamical Black Hole Spacetimes

Karanvir Singh

Submitted: June 29, 2021

Abstract

Many introductory texts on general relativity introduce event horizons as the defining feature of black holes. However such seemingly benign constructs have some key physical limitations. Therefore, it is imperative to construct horizons which accurately describe the black hole region in spacetime and that can be used to extract physical properties and not act as merely well defined mathematical constructs. In this thesis we shall discuss the event horizon and its shortcomings. We also review the laws of black hole mechanics and 'quasi-local' horizons that may be seen as alternatives to the event horizon. The laws of black hole mechanics in quasi-local horizons shall be examined. We also present numerical simulations of linear uniformly accelerated trajectories and find the corresponding Rindler horizons in Schwarzschild and Vaidya spacetimes. This thesis will attempt to persuade the reader that event horizons are a useful but limited way to understand the black hole region and that the quasi-local models can offer an elegant and physically insightful alternative. We also derive acceleration bounds for linear uniformly accelerated trajectories in Schwarzschild and Vaidya spacetimes.

Acknowledgement

I would like to thank Professor Alex B. Nielsen for invaluable discussion, encouragement and support throughout the duration of this project and express gratitude for his insight and help. This project would not have been possible without his expertise and guidance. Also, a huge thanks to all the staff at the Department of Mathematics and Physics at the University of Stavanger who have helped me along the way. Thank you to my family and partner for their unwavering moral support, especially during these strange and unpredictable times. Last, but certainly not least, I thank Sri Akal Purakh Ji for my spiritual, physical and mental well-being.

Contents

1 INTRODUCTION

Black holes are astrophysical phenomena of significant importance to the study of general relativity and quantum gravity. They are in some sense the most extreme consequence of general relativity with a strong gravitational field in a relatively compact region. If a working theory of quantum gravity is to be developed then it must tackle the black hole issue. Ever since the laws of black hole mechanics and Hawking radiation were published [1] [2] there appears to be a tantalising link between gravity and quantum physics. In fact one of the greatest achievements of string theory was to count the string microstates of a black hole and reproduce the celebrated Bekenstein-Hawking entropy [3].

In classical relativity, the event horizon is often seen as the defining boundary region of a black hole. According to Hawking and Ellis the event horizon is the *boundary of causal past of future null infinity* [4]. This notion has had great success in the early study of stationary black holes. However, there are numerous issues that arise from the classical definition of an event horizon. This thesis examines the various properties of the event horizon which have led many in the general relativity community to express serious doubt as to the suitability of the event horizon to define a black hole region [5]. Naturally, many have realised the drawbacks of the classical definition of an event horizon such as their global and teleological properties necessitates the search for 'quasi-local' alternatives. The difference between local and quasi-local is somewhat vague in the literature but essentially a local property refers to those at an exact point in spacetime. Whereas, quasi-local refers to a small finite region of spacetime [6]. These quasi-local horizons do away with the global issues associated with the event horizon. Interestingly, quasi-local horizons have their own laws of mechanics which arise naturally from them. Quasi-local horizon is a catch all term which encompasses a range of different horizons each with their own merit: trapping horizons, isolated horizons, dynamic horizons etc. There remains little agreement as to which quasi-local horizon is best for defining the black hole region, yet most of these quasi-local horizons depend on the notion of trapped surfaces as defined by Penrose [7]. Event horizons coincide with quasi-local horizons in stationary spacetimes, but the difference between the two becomes most apparent in the case of dynamical black hole spacetimes, which are still not well understood.

Of course the question remains, what exactly is a black hole? This is a seemingly simple question that one may expect has an equally simple answer. However, physicists from various subfields will give different responses as to what a black hole exactly is and where it 'begins' [5]. The popular notion in classical relativity is that a black hole is a region of spacetime with a gravitational field so strong that not even photons can escape from it. In order to refine this notion, Hawking and Ellis essentially defined the the black hole region as a 'region of no-escape' with the event horizon as its

boundary (hence the definition they espoused above). To obtain a full understanding of a black hole and what it exactly is would require a complete theory of quantum gravity that can explain the singularity at the core of a black hole. Such a theory remains elusive. Therefore, the importance of understanding black holes accurately is of utmost importance. To the astrophysicist, black holes are the playing ground for some of the most powerful phenomena in the universe such as X-ray binaries and quasars. As previously mentioned, reproducing Bekenstein-Hawking entropy from string microstates is one of the key milestones of string theory. Also, the first ever detection of gravitational waves arose from a black hole binary merger [8]. It is clear the study of black holes and its immediate relevance to modern physics can not be understated.

In this thesis we also numerically explore the formation of Rindler horizons in Schwarzschild and linear Vaidya spacetimes. Causal null horizons such as the Rindler horizon are of special interest here due to their thermodynamic properties for example the Unruh effect, where by an accelerated observer is predicted to measure a temperature [9]. The generalised second law has also been proved for causal null horizons [10]. The conformal Killing horizon is an example of a quasi-local black hole horizon that is a causal null horizon . Therefore, it would be of interest to study the degree to which conformal Killing horizon, which have been shown to exhibit thermodynamic properties [11], inherit or exhibit the thermodynamic properties of the Rindler horizon.

This thesis is structured as follows: Chapter (2) discusses some of the historical development of black hole studies including a short discussion on the observational evidence for black holes. Chapter (3) discusses the standard definition of a black hole in terms of the event horizon and why exactly it is so problematic. Chapter (4) reviews the laws of black hole mechanics as they were originally formulated [1]. The quasi-local alternatives are then introduced in Chapter (5) and discussed whilst the laws of black hole mechanics for them are reviewed in Chapter (6). Finally, Chapter (7) discusses the Rindler trajectories in black hole spacetimes.

2 HISTORICAL DEVELOPMENTS

2.1 Coordinate Systems

We will discuss here the various solutions of the Einstein field equations that have been used historically to describe black hole spacetimes. The main aim in this chapter is to show the gradual process of generalisation which has led to the development of different notions of horizons in the context of black holes. We will encounter the Schwarzschild black hole with its event horizon being a single Killing horizon. Also the Reissner-Nordström black hole that has inner and outer horizons, with the inner horizon being a Cauchy horizon and the outer, an event horizon. The Kerr-Newman metric for rotating, charged axially symmetric black holes in vacuum gives rise to the ergosphere region, the boundary of which is a Killing horizon. Finally, dynamical black holes such as those described by the Vaidya metric, which permit dynamical horizons which are not event horizons.

The theoretical foundations for Black holes in modern physics date back to Karl Schwarzschild in 1915 who derived a solution to the Einstein field equations [12], now known as the Schwarzschild metric, which after some minor modification takes the form:

$$ds^2 = -(1 - \frac{2M}{r})dt^2 + (1 - \frac{2M}{r})^{-1}dr^2 + r^2 d\Omega^2 \tag{2.1}$$

Where $d\Omega^2 = d\theta^2 + sin^2\theta d\phi^2$ The Schwarzschild metric describes the gravitational field that arises when a spacetime contains a spherical mass in a vacuum. This exact solution assumes electric charge, angular momentum and cosmological constant are all zero. One notes that something rather interesting happens at the point $r = 0$ and $r = 2M$ where the metric components appear to 'blow up'. The exact physical importance of these coordinate points was not fully understood by relativists and would take later developments and refinement on the Schwarzschild metric to uncover. In fact, it was shown that $r = 2M$ is merely a consequence of the Schwarzschild coordinate system and that in Eddington-Finkelstein coordinates, $r = 2M$ does not blow up at the future black hole horizon (requires Kruskal-Szekeres coordinates to ensure it also does not blow up at the past white hole horizon). The Eddington-Finkelstein coordinates are constructed using radial null geodesics and a coordinate transformation with a 'tortoise' coordinate which results in a metric that does not exhibit any strange behaviour at $r = 2M$. In Eddington-Finkelstein coordinates inward/outward radial null geodesics define the surfaces of constant null time (u, v), while the radial coordinate r is the same that appears in Eq (2.1).

The tortoise coordinate r^*, is defined as:

$$r^* = r + 2Mln|\frac{r}{2M} - 1|. \tag{2.2}$$

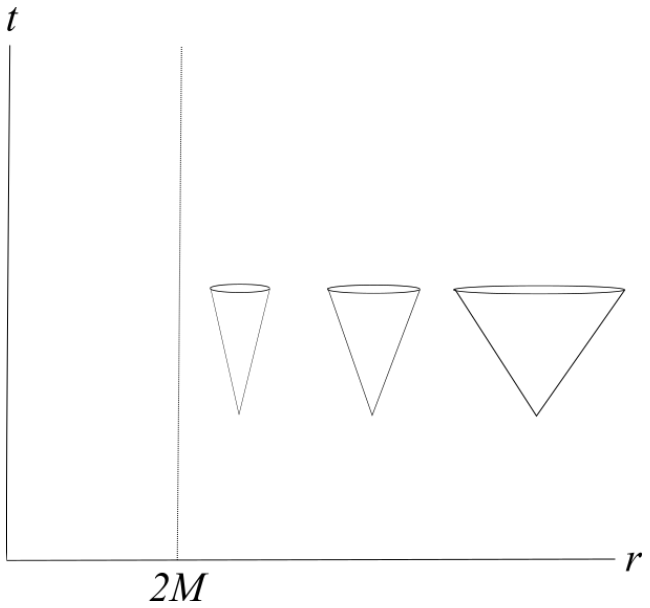

Figure 2.1: Spacetime diagram in Schwarzschild coordinates showing lightcones approach the surface $r = 2M$. Far away from $r = 2M$, the slope is ± 1 whilst as the lightcones approach $r = 2M$, $dt/dr \to \infty$, thus it appears as thought the lightcones close up.

Which satisfies the condition:

$$\frac{dr^*}{dr} = (1 - \frac{2M}{r})^{-1}. \tag{2.3}$$

The Einstein equations can then be solved using $r*$ to find the solution. The 'outgoing' Eddington-Finkelstein metric, is constructed using the outgoing null coordinate via the transformation $u = t - r^*$, to obtain:

$$ds^2 = -(1 - \frac{2M}{r})du^2 - 2dudr + r^2 d\Omega^2. \tag{2.4}$$

Similarly for the ingoing null coordinate, the following transformation applies: $v = t + r^*$, which gives:

$$ds^2 = -(1 - \frac{2M}{r})dv^2 + 2dvdr + r^2 d\Omega^2. \tag{2.5}$$

Martin Kruskal and George Szekeres both independently arrived at a coordinate system which bears their names, the Kruskal-Szekeres coordinates [13]. In this coordinate system, the resulting metric covers the entire spacetime manifold of the Schwarzschild solution.

To construct the Schwarzschild metric in Kruskal-Szekeres coordinates, the time coordinate in Schwarzschild coordinates t is replaced by a timelike coordinate T and

the radial component r is replaced by a spacelike coordinate X. The exterior black hole region, where $r > 2M$ is defined as:

$$T = (\frac{r}{2M} - 1)^{\frac{1}{2}} e^{\frac{r}{4M}} \sinh(\frac{t}{4M}). \tag{2.6}$$

$$X = (\frac{r}{2M} - 1)^{\frac{1}{2}} e^{\frac{r}{4M}} \cosh(\frac{t}{4M}). \tag{2.7}$$

Similarly for the interior Black Hole region $0 < r < 2M$:

$$T = (1 - \frac{r}{2M})^{\frac{1}{2}} e^{\frac{r}{4M}} \cosh(\frac{t}{4M}). \tag{2.8}$$

$$X = (1 - \frac{r}{2M})^{\frac{1}{2}} e^{\frac{r}{4M}} \sinh(\frac{t}{4M}). \tag{2.9}$$

Solving for the Schwarzschild radial component r:

$$r = 2M(1 + W_0(\frac{X^2 - T^2}{e})). \tag{2.10}$$

Where W_0 is the Lambert W function. Also, the Schwarzschild time component t, in the external region:

$$t = 4M \operatorname{arctanh}(\frac{T}{X}). \tag{2.11}$$

In the interior region:

$$t = 4M \operatorname{arctanh}(\frac{X}{T}). \tag{2.12}$$

The Schwarzschild metric can thus be expressed as:

$$ds^2 = \frac{32M^3}{r} e^{\frac{-r}{2M}} (-dT^2 + dX^2) + r^2 d\Omega^2. \tag{2.13}$$

Kruskal-Szekeres coordinates describe the *maximally extended* Schwarzschild solution. All radial null geodesics appear as 45°straight lines when drawn on the Kruskal diagram as $ds = 0$ which implies $dX = \pm dT$. One can also be motivated to introduce a variant on Kruskal-Szekeres coordinates closely related to Eddington-Finkelstein coordinates where outgoing and ingoing null geodesics are constant values. For outgoing null geodesics:

$$U = T - X \tag{2.14}$$

$$V = T + X \tag{2.15}$$

Thus, Eq (2.13) in null Kruskal coordinates becomes:

$$ds^2 = -\frac{32M^3}{r} e^{\frac{-r}{2M}} dU dV + r^2 d\Omega^2. \tag{2.16}$$

So outgoing null rays move along $U = constant$, whereas ingoing null rays move along $V = constant$. Surfaces of constant r are given by $UV = constant$. At the black hole singularity $r = 0$, $UV = 1$ and $r = 2M$ can be at $U = 0$ or $V = 0$.

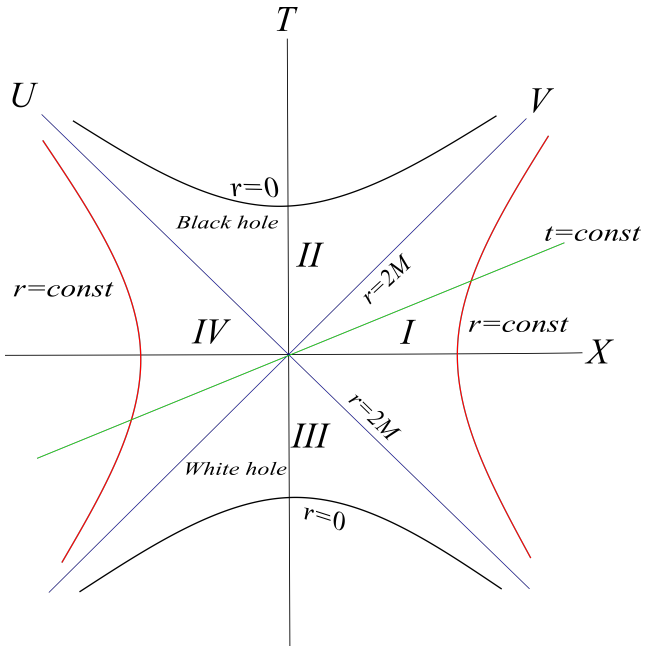

Figure 2.2: Kruskal-Szekeres diagram showing the maximally extended Schwarzschild solution. Lines of $t = constant$ are depicted as straight lines. Lines of $r = constant$ are depicted as hyperbolae. There are four distinct regions of the Kruskal-Szekeres diagram. I) is the spacetime observable by physical instruments and for all intents and purposes represents our observable universe. It is defined by $-X < T < X$ and $r > 2M$. II) is the black hole region bounded by $r = 2M$. Infalling matter will fall to the singularity at $r = 0$. II) is defined as the region where $|X| < T < \sqrt{1 + X^2}$ and $0 < r < 2M$. III) is the region depicting the white hole spacetime. A white hole acts in an opposite way to the black hole: a region where signals can only escape from. It is defined by$-\sqrt{1 + X^2} < T < -|X|$ and $0 < r < 2M$. Finally, there is region IV) which has properties similar to I) and basically denotes an asymptotically flat spacetime. It is a parallel universe causally disconnected from I). It is defined by $X < T < -X$ and $r > 2M$.

2.2 Other Black Hole solutions

The Schwarzschild metric describes a stationary, spherically symmetric mass in a vacuum, this idealised scenario is obviously suited to only a few physical phenomena. It was imperative to find other solutions of the Einstein field equations that yield more generalised results. This section looks at the development of a few of these solutions and how the notion of *horizons* as applied to black hole became more generalised.

2.2.1 Reissner–Nordström metric

If a charged particle crosses the event horizon of a Schwarzschild black hole, the black hole becomes electrically charged. A black hole of non-zero electric charge implies the necessity to solve the Einstein-Maxwell equations to take into account the stress-energy tensor of the electromagnetic field. As the generalised Birkhoff theorem

is obeyed in the case of a spherically symmetric electric field, the metric must be of similar form to Eq (2.1). Solving the Einstein-Maxwell equations, one finds the metric to be given by:

$$ds^2 = -(1 - \frac{2M}{r} + \frac{Q^2}{r^2})dt^2 + (1 - \frac{2M}{r} + \frac{Q^2}{r^2})^{-1}dr^2 + r^2 d\Omega^2. \quad (2.17)$$

Where Q is the electric charge of the Black Hole. This is known as the Reissner–Nordström metric [14][15]. The function $(1 - \frac{2M}{r} + \frac{Q^2}{r^2})$ is zero at the coordinate point $r_\pm$, where:

$$r_\pm = M \pm \sqrt{M^2 - Q^2}. \quad (2.18)$$

r_+ is the event horizon where as the 'inner horizon' r_- is known as the *Cauchy horizon*. If $|Q| \leq M$ then Eq (2.18) has real roots and the spacetime contains a Reissner–Nordström Black Hole. There is something called a *naked singularity* at $r = 0$ if $|Q| > M$. The implications of such a singularity will be discussed below. If $|Q| = M$ then the solution is referred to as the extreme Reissner–Nordström Black Hole.

The naked singularity refers to a singularity that has no event horizon. If naked singularities are a physical reality then in principle they should be directly observable. However, it is generally thought that objects with a charge greater than their mass can not collapse to form a singularity (in principle they could still collapse to a very compact object). If they could, a naked singularity would result. By way of the *Weak cosmic censorship hypothesis* (WCC), naked singularities can not exist in our universe [16]. Yet WCC has been contested and it has been shown theoretically at least that naked singularities can potentially form in nature although they are unstable [17]. This idea has also been promoted very recently by Joshi [18]

2.2.2 Kerr Metric

The Schwarzschild metric was the second solution of the Einstein field equations, with the first being the trivial flat space case. As such, the Schwarzschild solution (and Reissner–Nordström) describe an exceedingly idealistic scenario of some constant mass with zero angular momentum and spherical symmetry (although Reissner–Nordström takes charge into consideration). A more general solution was found in 1963, courtesy of Roy Kerr [19]. In Boyer-Lindquist coordinates, the *Kerr metric* reads:

$$ds^2 = -(1 - \frac{2Mr}{\Sigma})dt^2 - \frac{4Mrasin^2\theta}{\Sigma}dtd\phi + \frac{Asin^2\theta}{\Sigma}d\phi^2 + \frac{\Sigma}{\Delta}dr^2 + \Sigma d\theta^2. \quad (2.19)$$

Where:

$$\Sigma = r^2 + a^2 cos^2\theta. \quad (2.20)$$

$$\Delta = r^2 - 2Mr + a^2. \quad (2.21)$$

$$A = (r^2 + a^2) - \Delta a^2 sin^2\theta. \quad (2.22)$$

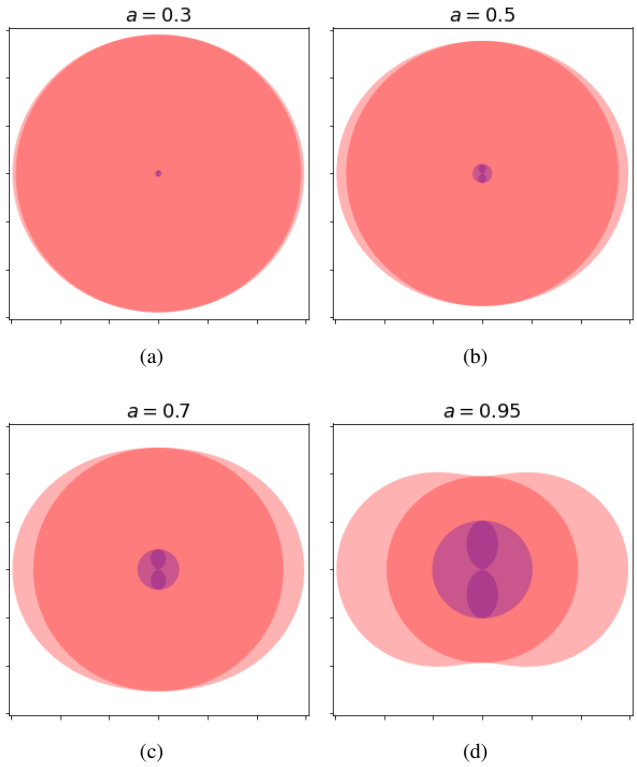

Figure 2.3: Diagrams showing the structure of the Kerr black hole for different values of a, the rotation parameter. Going radially inwards, the light pink area shows the outer ergoshpere, the dark pink area shows the outer horizon. Then we have the inner horizon denoted by light purple and then the inner ergosphere in dark purple. (a) $a = 0.3$. (b) $a = 0.5$. (c) $a = 0.7$. (d) $a = 0.95$. As $a \to 0$, we obtain a single surface that is the event horizon of a Schwarzschild black hole. We can see this clearly by setting $a = 0$, Eq (2.19) simply reduces to the Schwarzschild metric. As $a \to 1$ the inner ergosphere region begins to become more visible.

a is the rotation parameter, it has dimensions of length, the angular momentum $J = aM$. The Kerr metric can be further generalised to take describe a charged, rotating black hole. The resulting metric is known as the *Kerr-Newman metric*:

$$ds^2 = -(1-\frac{2Mr-Q^2}{\Sigma})dt^2 - \frac{(2Mr-Q^2)2asin^2\theta}{\Sigma}dtd\phi + \frac{Asin^2\theta}{\Sigma}d\phi^2 + \frac{\Sigma}{\Delta}dr^2 + \Sigma d\theta^2. \tag{2.23}$$

Where,

$$\Sigma = r^2 + a^2cos^2\theta. \tag{2.24}$$

$$\Delta = r^2 - 2Mr + a^2 + Q^2. \tag{2.25}$$

$$A = (r^2 + a^2) - \Delta a^2 sin^2\theta. \tag{2.26}$$

2.2.3 Ergospheres and Event Horizons in Kerr-Newman Metric

In the Kerr-Newman metric, the event horizon is given by:

$$r = M + \sqrt{M^2 - a^2 - Q^2}. \tag{2.27}$$

However, for rotating black holes there is another region that is of importance, the ergosphere. The ergosphere is an additional region that lies outside the event horizon. In the Schwarzschild metric, the surface of infinite redshift coincides with the event horizon. However, in a rotating black hole, this surface occurs at the boundary of the ergosphere, defined by the equation:

$$\Sigma - 2Mr = r^2 - 2Mr + a^2 cos^2\theta = 0. \tag{2.28}$$

Solving for r:

$$r = M + \sqrt{M^2 - a^2 cos^2\theta}. \tag{2.29}$$

This also happens to be a Killing horizon. More specifically, the region between the event horizon and infinite redshift surface is the ergosphere. An observer moving at constant r and $\theta = \pi/2$ can corotate with the Black hole [20]. Also, as the ergoshpere lies outside the event horizons it is possible to reach future null infinity i.e 'escape' from it. Via a process known as the *Penrose process*, it becomes possible to extract energy from the black hole [21].

2.3 Vaidya Metric

The Vaidya solution [22] [23] will be of utmost importance later on in this thesis and thus warrants an introduction. Considering once again, Eq (2.5):

$$ds^2 = -(1 - \frac{2M}{r})dv^2 + 2dvdr + r^2 d\Omega^2. \tag{2.30}$$

One can now allow the mass M to be a function of the advanced time coordinate v, thus Eq (2.5) becomes:

$$ds^2 = -(1 - \frac{2M(v)}{r})dv^2 + 2dvdr + r^2 d\Omega^2. \tag{2.31}$$

Similarly in the outgoing Eddington-Finkelstein coordinates:

$$ds^2 = -(1 - \frac{2M(u)}{r})du^2 - 2dudr + r^2 d\Omega^2. \tag{2.32}$$

The Vaidya solution is an exact solution of the Einstein equations for pressureless null dust, with stress energy tensor in ingoing Eddington-Finkelstein coordinates: $T_{ab} = \frac{dM/dv}{4\pi r^2} l_a l_b$, where $l_a = -\partial_a v$ It approximates a non-rotating black hole that is

emitting or absorbing matter. The Vaidya solution does not provide the entire picture of a black hole's lifetime. However, it has been used as tool to model dynamical black hole spacetimes in regimes close to the horizon [24][25]. We will encounter this metric again in Chapter (5) and (6) as part of the discussion on quasi-local horizons. It will also feature extensively in Chapter (7) where it is used as one of the background spacetimes to model linear uniformly accelerated trajectories.

2.4 Later Developments

In 1958, David Finkelstein argued the coordinate point $r = 2M$ is not a true physical singularity but acts as what he called a *perfect unidirectional membrane*: a boundary where observers can only cross over in one direction, more popularly known as an event horizon. [26]. The notion of event horizons will be discussed more thoroughly in Chapter (3), where its various physically bizarre properties and implications are discussed.

Further work, by Hawking, Carter and Bardeen in the 1960s and 1970s led to the formulation of black hole thermodynamics [1], whereby black holes appeared to work in close analogy to the laws of thermodynamics (see Chapter (4) for further discussion), this was then later developed by Hawking who used Quantum Mechanics to predict 'Hawking Radiation' whereby black holes are expected to radiate as black bodies [2]. Hawking was able to arrive at this remarkable result by considering the black hole's affect on the background vacuum. As the vacuum is unstable in the presence of a black hole of mass M, it decays and would appear as though the black hole emits radiation. By studying the quantum field effects in a black hole spacetime, Hawking was able to arrive at the following relation for thermal radiation from the black hole:

$$T_H = \frac{\hbar c^3}{8\pi G k_B M}. \tag{2.33}$$

This is known as the *Hawking temperature*. This thesis uses $c = G = \hbar = k_B = 1$, but the constants have been reintroduced in Eq (2.33) to outline specifically how the study of black holes motivates the desire to find some connection between the quantum effects that govern the radiation that occurs in the presence of a strong gravitational field.

The prediction that black holes radiate thermally soon led to the development of the 'Information Paradox' [27]. For a classical black hole, matter that has the unfortunate fate of crossing the event horizon, can no longer influence anything outside the event horizon. To external observers the matter would have appeared to have disappeared forever. However, when we consider the quantum effects near the event horizon, the situation appears different due to Hawking radiation. Eq (2.33) tells us that black holes radiate at a temperature, $T \propto 1/M$. The black hole is theorised to evaporate until it reaches its final state which is pure thermal Hawking radiation. The calculation of Von Neumann entropy in this this scenario, tells us that there is a Von Neumann entropy

$\propto M^2$. For there to be unitary evolution, quantum mechanics requires there to be a constant Von Neumann entropy. This seems to suggest that either quantum mechanics is violated in black hole evaporation or that new physics is required to account for this. Solutions to the information paradox have been proposed, but there remains debate on the validity of these [28] [29].

2.5 Observational Evidence for Black Holes

Direct observations of black holes is of course not a straightforward matter. Other than hypothesised Hawking radiation, black holes are not expected to emit any electromagnetic radiation. However, this has not harmed the motivation of astrophysicists to search for black holes in any way. In fact, certain astrophysical observations have been made since the 1970s that appear to be best explained by a black hole. The observational evidence of black holes is not the core theme of this thesis, yet it is important to note briefly that there is a wealth of astrophysical evidence for black holes that includes X-ray binaries [30] and S-stars in Sagittarius A* [31]. Merging binary black holes led to the first detection of gravitational waves [8] and consequently, the Nobel Prize for Physics 2017 was awarded to Weiss, Thorne and Barish for their contributions to LIGO [32]. More recently, the Nobel Prize for Physics 2020 was co-awarded to Penrose 'For the discovery that black hole formation is a robust prediction of the general theory of relativity'. Whilst the other half was awarded jointly to Genzel and Ghez for 'the discovery of a supermassive compact object at the centre of our galaxy' [33].

3.1 What is the Event Horizon?

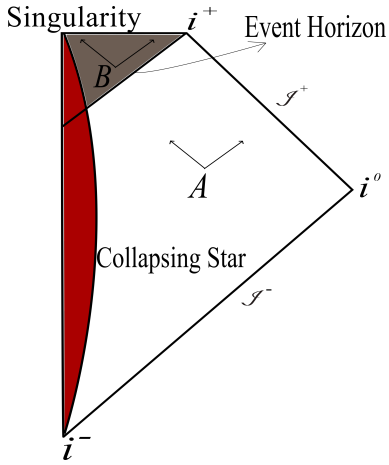

Figure 3.1: A Carter-Penrose diagram showing the collapse of a star to form a black hole and the formation of the event horizon region in the corresponding spacetime. Past and future null infinity is represented by $\mathscr{I}^-$ and $\mathscr{I}^+$ respectively. Also, spacelike infinity at i^0 and past and future timelike infinities at i^- and i^+ respectively. We can see the boundary between the interior black hole region and exterior spacetime, demarcates the event horizon. The red shell shows a star collapsing to form a black hole.

As previously mentioned, an event horizon has been defined as the boundary of causal past of future null infinity [4]. This definition attempts to make precise the idea of a black hole being a region of 'no escape'. Intuitively one can understand this by considering a region of spacetime exterior to the black hole whereby causal signals can in principle escape to infinity. Secondly, there is the interior black hole region where in principle causal signals cannot escape from. The event horizon is thus the boundary of the two. An event horizon is a null hypersurface (a hypersurface whose normal vector at every point is a null vector). Also, event horizons can be defined for a certain class of accelerated observers in a Minkowski spacetime [4]. Using conformal mappings which allow compactification of spacetimes of interest, we can construct pictorial boundaries out to infinity for null, spacelike and timelike curves. An example of such a conformal mapping is given by the Carter-Penrose diagram in Figure (3.1). With past and future null infinity represented by $\mathscr{I}^-$ and $\mathscr{I}^+$ respectively, spacelike infinity at i^0 and past and future timelike infinities at i^- and i^+ respectively. In this conformal mapping one can see that a region of spacetime contains a black hole if there are regions where null curves can not escape to $\mathscr{I}^+$.

If we are to use the standard definition for event horizons à la Hawking and Ellis,

then one needs the entire future spacetime of the universe in order to simply locate it, as event horizons simply by definition depends on the structure of spacetime out to infinity. This makes them quite limited if they are to be considered the defining feature of a black hole region. An astute reader will realise that such definitions do not rely on any locally identifiable fields or intrinsic properties of the black hole, rather they depend on the future outcome of null curves thus being teleological. Also as the event horizon is founded upon the *global causal structure* of spacetime it requires knowledge of spacetime out to null infinity simply to locate it.

A fascinating consequence of this non-locality is discussed by Ivan Booth [34] whereby the case of matter falling into the black hole is considered. One would naively expect that the event horizon should expand as the matter falls in. However, it would appear that the event horizon expands before any matter crosses the event horizon-hence the teleological nature of black holes. The growth ceases once all interactions between the event horizon and its surroundings come to a permanent halt.

A close inspection of the Raychaudhari equation and the focusing theorem that arises from it will aid in understanding this property of the event horizon. The Raychaudhari equation describes the expansion of congruences (systems of non-intersecting geodesics). The event horizon of course is defined as a null hypersurface so it can be equated with a congruence of null geodesics. The Raychaudhari equation for null geodesics is:

$$\frac{d\theta_{(l)}}{d\lambda} = -\frac{1}{2}\theta_{(l)}^2 - \sigma_{(l)ab}\sigma_{(l)}^{ab} - 8\pi T_{ab}l^a l^b. \tag{3.1}$$

Where l^a is some null vector that is tangent to the null congruence λ is some affine parameter. σ is the shear tensor and T_{ab} is the Stress-Energy tensor. The expansion θ can be considered as the fractional change in transverse area form, A with respect to λ:

$$\theta_{(l)}A = \frac{dA}{d\lambda}. \tag{3.2}$$

Eq (3.1) tells us that the first two terms will always be negative. Furthermore the null energy condition implies that $T_{ab}l^a l^b \geq 0$. So Eq (3.1) tells us that for congruences of null geodesics, $\frac{d\theta_{(l)}}{d\lambda} \leq 0$. For an initially converging congruence of null geodesics where $\theta_{(l)} < 0$ and as a consequence of the focusing theorem the congruence will converge even more rapidly in the future. So for some initially converging congruence, the focusing theorem tells us that $\theta_{(l)} \to -\infty$ in some finite time. Thus a congruence of initially converging null geodesics forms a caustic within finite time. For an event horizon that asymptotes to a stationary spacetime, $\theta_{(l)} \geq 0$. This can be further understood by substituting Eq (3.2) into Eq (3.1):

$$\frac{d^2A}{d\lambda^2} = (\frac{1}{2}\theta_{(l)}^2 - \sigma_{(l)ab}\sigma_{(l)}^{ab} - 8\pi T_{ab}l^a l^b)A. \tag{3.3}$$

Booth then considers the case where two spherical shells collapse to form a black hole [34], assuming the outermost shell is Schwarzschild and static. When collapse begins and the two shells collapse within $r = 2M$, we know that is where their event horizon is. The evolution of this surface can be traced back in time to find its origin at $r = 0$. Thus, the event horizon appears in anticipation of future events and $\theta_{(l)}$ will posses its largest value. Eq (3.3) then steers the evolution as one proceeds in time. Assuming the horizon forms in a vacuum, Eq (3.3) tells us that $dA/d\lambda > 0$ and $d^2A/d\lambda^2 > 0$ when the horizon is newly formed. Then a shell of matter crosses the horizon and causes the rate to decrease, until it is almost zero. When the horizon returns to vacuum, its growth again begins to accelerate. The second shell of matter then crosses causing $\theta_{(l)} \to 0$ and the horizon to reach its maximum area.

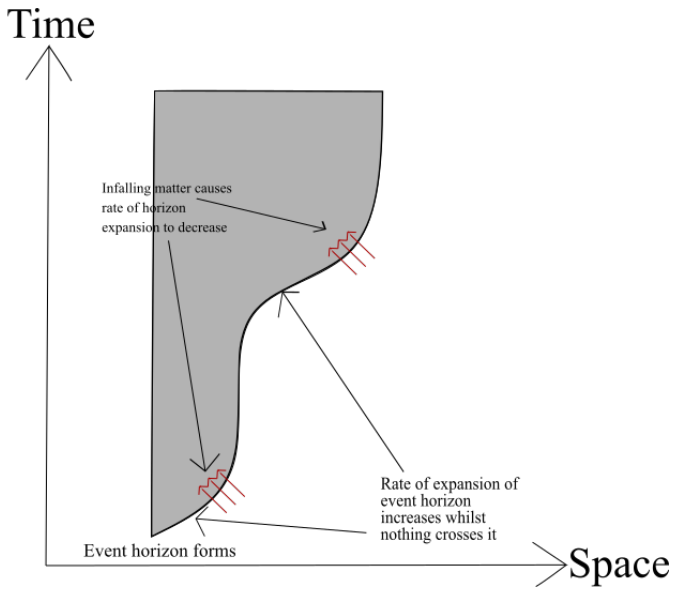

Figure 3.2: Collapse of two concentric, spherically symmetric shells of matter to form a black hole region with highly non causal properties. The red lines display matter flux. Adapted from [34]

3.1.1 The Schrodinger Black Hole

In [35], the case of a Schrodinger black hole is discussed which further exemplifies the strange behaviour of the event horizon of a black hole. In a manner analogous to the infamous Schrodinger's cat thought experiment, Sudarsky discusses the potential for a device that makes the random choice to begin the collapse of a shell of matter to within its Schwarzschild radius. The exact considerations shall be discussed in this subsection.

Imagine a shell of two thin massless concentric spherical walls separated by small distance that reflect the electromagnetic radiation confined between them. There is

some device that triggers the collapse of this shell to form a black hole. The probability that a collapse is triggered is given by p whilst the probability of there being no collapse is simply given by $q = 1 - p$. For $r \geq r_{shell}$ the metric is Schwarzschild:

$$ds^2 = -(1 - \frac{2M}{r})dt^2 + (1 - \frac{2M}{r})^{-1}dr^2 + r^2 d\Omega^2. \tag{3.4}$$

For $R \leq r_{shell}$ the metric is Minkowskian:

$$ds^2 = -dT^2 + dR^2 + R^2 d\Omega^2. \tag{3.5}$$

Specifying the shell's motion by functions of (t, r) and (T, R) respectively: $r_{shell} = \rho^{(1)}(t)$ and $R_{shell} = \rho^{(2)}(T)$. We can then express the exterior and interior metric respectively as:

$$d\sigma^2 = -[(1 - \frac{2M}{r}) - (1 - \frac{2M}{r})^{-1}(\frac{dr}{dt})^2]dt^2 + r^2 d\Omega^2. \tag{3.6}$$

And:

$$d\sigma^2 = -[1 - (\frac{dR}{dT})^2]dT^2 + R^2 d\Omega^2. \tag{3.7}$$

Relating the interior and exterior coordinates so that:

$$-[(1 - \frac{2M}{r}) - (1 - \frac{2M}{r})^{-1}(\frac{dr}{dt})^2]dt^2 = -[1 - (\frac{dR}{dT})^2]dT^2. \tag{3.8}$$

The time where the device makes triggers the collapse is set to $t = T = 0$. When $t < 0$ and $T < 0$, the shell is static with initial radius $R = R_0$. Eq (3.8) tells us that:

$$T = \sqrt{1 - \frac{2M}{R}}t. \tag{3.9}$$

If the shell begins to collapse at $t = T = 0$ then, one find T and t as functions of R. For the left hand side of Eq (3.8):

$$R(t) = R_0 - 2M \log(\frac{R(t) - 2M}{R_0 - 2M}) - t. \tag{3.10}$$

Also for the right hand side:

$$R(T) = R_0 - T \tag{3.11}$$

Eq (3.10) tells us that $R(t) = 2M$ at $t = +\infty$, whilst Eq (3.11) tells us that $T = R_0 - 2M$. Of course, the event horizon must form before this. To find when exactly the event horizon forms Sudarsky considers the case of a radial null ray emanating from the centre of the shell travelling outwards, beginning at $T = T_1$. This null ray can only reach future null infinity if it reaches $R = 2M$ before collapse. The signal travels outward with $R = T - T_1$. Where it reaches the shell at: $T = \frac{1}{2}(R_0 + T_1)$ where

the radius of the shell becomes $R_{shell} = \frac{1}{2}(R_0 - T_1)$. The shell can escape if we set $R_{shell} = 2M$, thus finding $T_1 < R_0 - 4M$. This is another example of the teleology of event horizons. The location of the horizon at times before $T = 0$, depends on what happens later at $T = 0$.

Therefore it seems as though event horizons possess at least two strange unphysical properties namely:

1. They appear to be highly non-local objects that require spacetimes with well defined $\mathscr{I}^+$. Identification of the event horizon region requires knowledge of the spacetime out to infinity, making any local observation impossible.
2. They display strange teleological behaviour whereby it appears as though the horizon area increases before matter crosses it.

The exotic nature of the behaviour of black holes may indeed suggest that local identification of a black hole region is physically impossible if event horizons are the correct way to approach them. However, this is not necessarily the case as 'Quasi-local' alternatives to the event horizon have been suggested.

3.2 Killing Horizons

Before introducing quasi-local alternatives to the event horizon, it is important to consider the case of stationary, static black hole spacetimes that permit *Killing horizons*. If some vector field χ^μ, satisfies the Killing equations:

$$\nabla_\mu \chi_\nu + \nabla_\nu \chi_\mu = 0. \tag{3.12}$$

Then χ^μ is said to be a *Killing vector field*.The Killing horizon, Σ, is the null hypersurface tangential to χ^μ at all points in the spacetime, given $\chi^\mu \chi_\mu = 0$ on Σ. In the idealised case of static black hole spacetimes, where there is future null infinity, the event horizon coincides with the Killing horizon.

The presence of a Killing horizon was used in [1] to formulate a black holes' surface gravity, which gave rise to the celebrated laws of black hole thermodynamics. In the Schwarzschild spacetime, the line element given by Eq (2.1) holds and for the timelike Killing vector $\chi^\mu = (\partial/\partial t)^\mu$ in the region where $r > 2M$ becomes null when $r = 2M$. Generalising upon this, any event horizon in a static, stationary spacetime is a Killing horizon for $\chi^\mu = (\partial/\partial t)^\mu$ [36].

But in the case where there is a non-static, stationary and asymptotically flat spacetime then the event horizon is a Killing horizon for a Killing vector that is a linear combination of time and rotational symmetries:

$$\chi^\mu = (\partial/\partial t)^\mu + \Omega(\partial/\partial \phi)^\mu. \tag{3.13}$$

Where Ω is the angular velocity at the horizon. It is imperative to note that the Killing horizon does not define dynamical spacetimes which would coincide in the physical cases of black hole accretion, binary black hole mergers etc. Therefore the laws of black hole mechanics are formulated for an idealised case (with the exception of the second law which still works in dynamical cases, but more on that later). The basis of equating the stationary Schwarzschild event horizon with a localised Killing horizon lies in the *strong rigidity* theorem of Hawking [37]. The theorem asserts that if the weak energy condition is satisfied by the stress-energy tensor and matter obeys well behaved hyperbolic equations, the global and teleological event horizon can be recast as a Killing horizon. The concept of 'conformal' Killing horizons is also introduced in Chapter (5).

3.3 Rindler Horizons

It is of interest to note that there exist horizons in Minkowski flat space that are not associated with strong gravitational fields. The Rindler horizon is such an example [38] that arises due to accelerated observers in Minkowski flat space that undergo hyperbolic motion. The Rindler horizon is effectively the boundary of spacetime beyond which it is impossible to send signals to the accelerating observer. Hyperbolic motion of linear uniformly accelerated observers in black hole spacetimes and the Rindler horizons they form are discussed in greater depth in Chapter (7).

4 BLACK HOLE MECHANICS

4.1 Preliminaries

This section presents a review of the laws of Black hole mechanics that have been formulated using the Killing horizon by Bardeen et al. [1][23]. Using the event horizon's tangential vectors for some coordinates on the horizon $y^\alpha = (v, \theta^A)$, where v is the advanced time coordinate and θ^A is the null generators, Bardeen et al. were able to arrive at their celebrated laws of black hole mechanics. The horizon's tangential vectors read:

$$\chi^\alpha = (\frac{\partial x^\alpha}{\partial v})_{\theta^A} \tag{4.1}$$

$$e^\alpha_A = (\frac{\partial x^\alpha}{\partial \theta^A})_v. \tag{4.2}$$

Where the Lie derivative of Eq (4.2) along χ satisfies:

$$\mathcal{L}_\chi e^\alpha_A = \chi^\alpha e^\alpha_A = 0. \tag{4.3}$$

Stationary black holes must be static or axially symmetric. These symmetry considerations imply two Killing vectors, t^α and ϕ^α for stationary spacetime. Hawking was able to arrive at a linear combination of these Killing vectors which is null at the event horizon:

$$\chi^\alpha = t^\alpha + \Omega_H \phi^\alpha. \tag{4.4}$$

So in the case of stationary spacetimes, the event horizon is a Killing horizon (as we have seen in Chapter (3)). The 'surface gravity' of the black hole, as we will see, is defined via the following acceleration relation:

$$\chi^\beta \nabla_\beta \chi^\alpha = \kappa \chi^\alpha. \tag{4.5}$$

4.2 Zeroth Law of Black Hole Mechanics

The Zeroth Law states simply that: *Surface gravity κ of a stationary black hole is constant over the event horizon.* This was shown to be true for the Kerr metric by Carter [39], but I shall present the version which holds for all types black holes. In order to show that κ is constant over the event horizon, two criteria must be met:

1. κ is constant along the event horizon's null generators.
2. κ does not vary from generator to generator

The surface gravity, κ is given, in terms of Killing vectors,χ as: $\kappa^2 = -\frac{1}{2}\chi^{\mu;\nu}\chi_{\mu;\nu}$. Differentiating this in a direction tangential to the event horizon whilst using the identity: $\chi_{\alpha;\mu\nu} = R_{\alpha\mu\nu\beta}\chi^\beta$, one obtains:

$$2\kappa\kappa_{,\alpha} = -\chi^{\mu;\nu} R_{\mu\nu\alpha\beta}\chi^{\beta}. \tag{4.6}$$

κ is constant following from:

$$\kappa_{,\alpha}\chi^{\alpha} = 0. \tag{4.7}$$

Next is to examine the way in which κ varies in the transverse direction. (4.6) tells us that:

$$2\kappa\kappa_{,\alpha} e^{\alpha}_{A} = -\chi^{\mu;\nu} R_{\mu\nu\alpha\beta} e^{\alpha}_{A}\chi^{\beta}. \tag{4.8}$$

To show that the right hand side is zero, the assumption is made that the event horizon is geodesically complete, meaning $\chi^{\alpha} = 0$ contains a bifurcation 2-sphere so $\kappa_{,\alpha}e^{\alpha}_{A} = 0$ on the bifurcation 2-sphere. $\kappa_{,\alpha}e^{\alpha}_{A}$ is constant along all null generators on the event horizon and is zero on cross sections where $v =$ constant i.e. the event horizon. Ergo the value of κ does not change as one moves along the event horizon as it is uniform across its generators.

4.3 First Law of Black Hole mechanics

The first law of black hole mechanics can be expressed as:

$$\delta M = \frac{\kappa}{8\pi}\delta A + \Omega_H \delta J. \tag{4.9}$$

This gives an expression for the change in mass M, area A and angular momentum J. In order to arrive at this one needs to generalise Smarr's formula [40]. Assuming a stationary and axially symmetric black hole, the Komar expressions [41] for total mass and angular momentum are:

$$M = -\frac{1}{8\pi}\oint_{S} \nabla^{\alpha} t^{\beta} dS_{\alpha\beta} \tag{4.10}$$

$$J = \frac{1}{16\pi}\oint_{S} \nabla^{\alpha} \phi^{\beta} dS_{\alpha\beta}. \tag{4.11}$$

Here, the Komar expression are equivalent to the Hamiltonian definitions for mass and angular momentum for stationary and axially symmetric spacetimes. Where t^{β} is a timelike Killing vector and ϕ^{β} is the rotational Killing vector. Integrating over closed 2-surfaces, one can employ Gauss' theorem to express Eq (4.10) as an integral over a spacelike hypersurface Σ spanning the event horizon to spatial infinity:

$$M = M_H + 2\oint_{\Sigma} (T_{\alpha\beta} - \frac{1}{2}T g_{\alpha\beta}) n^{\alpha} t^{\beta} \sqrt{h} d^3 y \tag{4.12}$$

$$J = J_H + 2\oint_{\Sigma} (T_{\alpha\beta} - \frac{1}{2}T g_{\alpha\beta}) n^{\alpha} \phi^{\beta} \sqrt{h} d^3 y. \tag{4.13}$$

M_H and J_H are the black hole's mass and angular momentum, respectively. They are evaluated over $\mathcal{H}$ the inner boundary of Σ with outer boundary S:

$$M_H = -\frac{1}{8\pi}\oint_{\mathcal{H}} \nabla^\alpha t^\beta dS_{\alpha\beta} \tag{4.14}$$

$$J_H = -\frac{1}{16\pi}\oint_{\mathcal{H}} \nabla^\alpha \phi^\beta dS_{\alpha\beta}. \tag{4.15}$$

$dS_{\alpha\beta}$ is the two dimensional surface element. Looking at Eq (4.12), one can immediately see what these equations are telling us: total mass M given by the black hole contribution M_H and a contribution from the energy-matter distribution outside the black hole given by the second term. This interpretation also applies for J and J_H. If one assumes a vacuum around the black hole then $M = M_H$ and $J = J_H$. Putting Eq (4.14) and (4.15) together:

$$M_H - 2\Omega_H J_H = -\frac{1}{8\pi}\oint_{\mathcal{H}} \nabla^\alpha (t^\beta + \Omega_H \phi^\beta) dS_{\alpha\beta} \tag{4.16}$$

$$= -\frac{1}{8\pi}\oint_{\mathcal{H}} \nabla^\alpha \chi^\beta dS_{\alpha\beta} \tag{4.17}$$

$$= -\frac{1}{4\pi}\oint_{\mathcal{H}} \chi^{\beta;\alpha}\chi_\alpha N_\beta dS_{\alpha\beta}. \tag{4.18}$$

After some algebra and using the fact that $\chi^\alpha_{;\beta}\chi^\beta = \kappa\chi^\alpha$,where N^α is an auxiliary normalised null vector such that $N_\alpha\chi^\alpha = -1$ and the implication via the first law that κ is constant over the event horizon, this becomes:

$$\frac{\kappa}{4\pi}\oint_{\mathcal{H}} dS. \tag{4.19}$$

This integral simply reduces to the surface area of the horizon, A, so M_H simply becomes:

$$M_H = 2\Omega_H J_H + \frac{\kappa A}{4\pi}. \tag{4.20}$$

This is the generalised Smarr formula.

Next, consider a quasi-static process whereby a stationary black hole gains some mass so that its initial mass M goes to $M+\delta M$. Similarly the initial angular momentum J goes to $J + \delta J$ whilst A goes to $A + \delta A$. A relationship is then given from Smarr's formula for δM, δJ and δA :

$$\delta M = \frac{\kappa}{8\pi}\delta A + \Omega_H \delta J. \tag{4.21}$$

4.4 Second Law of Black Hole Mechanics

The second law states that the area of a black hole can never decrease given that the null energy condition holds: $\delta A \geq 0$. This was discovered by Hawking in 1971. It was largely derived via considering the focusing theorem that arises when one uses the Raychaudhari equation. As before, the expansion of a null congruence of in-going geodesics is given by:

$$\Theta_{(l)} = \frac{1}{A}\frac{dA}{d\lambda}. \tag{4.22}$$

The null Raychaudhari equation states that the rate of change for the expansion for such null congruences is:

$$\frac{d\theta_{(l)}}{d\lambda} = -\frac{1}{2}\theta^2_{(l)} - \sigma_{(l)ab}\sigma^{ab}_{(l)} - 8\pi T_{ab}l^a l^b. \tag{4.23}$$

Assuming the Null energy condition is satisfied then $8\pi T_{ab}l^a l^b > 0$. Therefore the RHS of Eq (4.23) is negative:

$$\frac{d\Theta}{d\lambda} \leq 0. \tag{4.24}$$

This is the same consideration as in the previous section whereby we arrived at the conclusion that gravity must always focus rays of light. If one assumes a null congruence of geodesics outside the event horizon where $\Theta < 0$. Then by the Raychaudhari equation, $\Theta \to -\infty$ in finite time, thus implying the light rays hit a singularity or intersect one another. However, the event horizon is defined as the future boundary of null infinity so light rays cannot intersect in the future direction. Ergo, $\Theta \geq 0$ on the event horizon.

4.5 Third Law of Black Hole Mechanics

The third law simply states that κ can not be reduced to zero in finite time assuming the weak energy condition is satisfied and if there is a bounded stress energy tensor. This was not shown in detail in [1], where Bardeen et al. argued for the third law intuitively. A detailed mathematical proof arose later given by Israel [42]

4.6 Generalised Second Law

Due to quantum effects near the event horizon, where by evaporation of the black hole reduces the area, it would appear the Second law of back hole mechanics is violated. However, black hole evaporation implies an increase in the entropy in the space surrounding the black hole. This motivated the concept of *Generalised entropy* [43] [20] the sum of entropy of the black hole,S_B and the immediate exterior region S_O:

$$S = S_B + S_O. \tag{4.25}$$

Considering the rate of mass and entropy increase in the black hole's exterior region due to Hawking radiation of some massless spin s field, as well as a non-rotating black hole's change in entropy, and comparing the resulting equations, allowed Zurek [44] to

numerically show that the generalized entropy must increase. Rate of increase of mass in the exterior black hole region is given by:

$$\frac{dM_O}{dt} = -\frac{dM}{dt} = \frac{1}{4}\sigma_s h_s \Sigma T_H^4. \tag{4.26}$$

Whilst the rate of increase of the entropy is given by:

$$\frac{dS_O}{dt} = \frac{1}{3}\sigma_s h_s \Sigma T_H^3. \tag{4.27}$$

Where $\sigma_s = \frac{\pi^2}{30}$ for bosons and $\frac{7\pi^2}{240}$ for fermions, h_s is the number of polarisations of the radiating field. Σ is the cross-section of the black hole, and T_H is the Hawking temperature.B_s is the dimensionless coefficient of order of unity. The change in entropy of a non rotating black hole is given via:

$$dS_B = T_H^{-1} dM. \tag{4.28}$$

Zurek compares Eq (4.26), (4.27) and (4.28) to arrive at:

$$-\frac{dS_O}{S_B} = \frac{4}{3}B_s. \tag{4.29}$$

Zurek was able to numerically show that $B_s > \frac{3}{4}$. Thus implying that the generalised entropy always increases for the case of an isolated non rotating black hole. Ergo, the generalised second law for black holes states that the generalised entropy of a black hole does not decrease:

$$\Delta S = \Delta S_B + \Delta S_O \geq 0. \tag{4.30}$$

4.7 Significance of the Black Hole Laws

One can see that these laws of black hole mechanics are strikingly analogous to the classical laws of thermodynamics where $\kappa/2\pi$ plays the role of temperature, $A/4$ the entropy and M appearing similar to the internal energy. The nature of this apparent coincidence was poorly understood but, Hawking was able to show that by considering the effects of quantum fields near the event horizons, then there is indeed a thermal flux of particles from the black hole region and that black holes do behave as thermal bodies due to quantum effects in strong gravitational fields [2]. This implies the existence of statistical mechanics of gravitational degrees of freedom which is interpreted by many as a signpost to a yet unknown theory of gravity.

5 QUASI-LOCAL HORIZONS

This section now presents some of the alternative 'Quasi-local' horizons that have been suggested as alternatives to the event horizon. Horizons that are 'Quasi-local' do not exhibit the strange global or teleological properties that event horizons display as shown in previous sections.

5.1 Apparent Horizons

Apparent horizons do not depend on well-defined $\mathscr{I}^+$ and instead rely on the notion of trapped surfaces which in principle should be locally identifiable structures in the spacetime. Apparent horizons are introduced in this thesis as the first example of a truly *quasi-local* horizon, whereby they do not rely on the global structure of causal spacetime and do not possess the teleological properties of event horizons. To introduce the notion of apparent horizons, it makes sense to first take a look at *trapped surfaces* and how they relate to apparent horizons.

5.1.1 Trapped Surfaces

The concept of trapped surfaces was first used by Sir Roger Penrose [7]. In the popular stellar collapse model when matter contracts within $r = 2m$, a spacelike 2-sphere forms just outside the matter contained region. A sphere Penrose labelled the *trapped surface*. Penrose defines the trapped surface as a 'closed, spacelike, 2-surface' where congruences of future directed null geodesics orthogonal to it have negative expansion for all points on the surface. Closed in this context means compact with no boundary.

For some trapped surface S, the expansion, θ of the outgoing and ingoing directions respectively:

$$\theta_{(l)} = (g^{ab} + l^a n^b + l^b n^a)\nabla_a l_b < 0 \tag{5.1}$$

$$\theta_{(n)} = (g^{ab} + l^a n^b + l^b n^a)\nabla_b n_b < 0. \tag{5.2}$$

Where l^a and n^a are null directions denoting the outgoing and in-going directions respectively. To gain a more intuitive grasp of the trapping surface we can imagine a 2-sphere in regular Minkowski space where a congruence of null rays orthogonal to the surface can be either in-going or out-going. For our in-going case we have negative expansion and vice versa for the out-going case. A trapped surface is such a surface where both groups of orthogonal null geodesics converge. This provides a convenient description of strong gravitational fields where one can imagine the expansion of a congruence decreasing due to strong gravitational effects.

It is important to note that the mere existence of trapped surfaces implies the existence of a singularity (Penrose's Singularity theorem) which is not the case for event horizons. In the Kerr-Newman solutions of black holes, trapped surfaces are found within the outer event horizon but outside the inner event horizon area.

5.1.2 Link with Apparent Horizons

One can apply the principles of trapped surfaces to define the *apparent horizon*. The apparent horizon is the outermost *marginally outer trapped surface* on a given spacelike hypersurface. For a surface to be *marginally* trapped, it must have:

$$\theta_{(l)} = 0 \tag{5.3}$$

$$\theta_{(n)} < 0. \tag{5.4}$$

Here, Eq (5.3) tells us that the congruence of null out-going geodesics momentarily stop expanding outwards. Eq (5.4) fulfills the requirement for a black hole as opposed to a white hole. Taking the union of all the trapped points associated with a trapped surface for a Kerr-Newman black hole, the boundary of this region is called the apparent horizon. An interesting feature of the apparent horizon is that they depend upon which foliation one takes of the 3-surface with marginal surfaces. This dependence of the apparent horizon on foliation choice is discussed in [45], where non-symmetric foliations of a Schwarzschild spacetime do not permit the existence of an apparent horizon. In the case that the null energy condition is satisfied, $T_{ab}l^a l^{ab} \geq 0$, apparent horizons will always be found within the event horizon. Ergo, the apparent horizon is distinct from the event horizon. This distinction is highlighted when the apparent and event horizons do not coincide in the case of charged, non-rotating, spherically symmetric bodies (Reissner–Nordström) and in the Vaidya spacetime (the simplest spacetime permitting emission or absorption of null dust). This is also true in the Schwarzschild spacetime for static, perturbed black holes. Furthermore, in the standard description of stellar collapse to form a black hole, the event horizon forms before the apparent horizon. The apparent horizon and event horizon regions will then coincide at future null infinity. It is important to note to the reader, that there are indeed cases where the null energy condition does not hold. This is the case in Hawking radiation [46]. Also, there are alternative theories of gravity such as Brans-Dicke [47], where the Brans-Dicke model of stellar collapse suggests that the apparent horizon lies outside the event horizon.

5.2 Trapping Horizons

We see in Chapter (3), that the event horizon is a fundamentally global and teleological in nature. This problem was realised quite early on in the history of black hole physics [4]. Developing Penrose's notion of a *Trapped surface*, i.e. a closed, spacelike, 2-surface, S, where the expansion of null geodesics is everywhere negative, Sean Hayward introduced a quasi-local analogue of future event horizons [48]. Hayward starts with Penrose's notion of a trapped surface and then looks at *future* trapped surfaces where the expansion of a pair of null normals l^a, n^a are both negative on S.

However, the trapping horizon is formulated on the basis of *marginal surfaces*, i.e. two-dimensional spacelike surface for which expansion of one of its null normals is zero. The future outer trapping horizon (FOTH) is therefore defined by Hayward as the closure of a three surface foliated by marginal surfaces that satisfies the following requirements:

1. Expansion of outgoing null normal to the surface, $\theta_{(l)} = 0$
2. $\theta_{(n)} < 0$
3. $n^a \nabla_a \theta_l < 0$

Conditions 1 and 2 encode the idea of this surface designating a black hole's surface. Condition 1 implies that instantaneously at the surface the expansion is zero. Condition 2 distinguishes the black hole region from a white hole. Condition 3 tells us that infinitesimal motion on in-going normals ensured the surface is outer so distinguishing outer horizons from inner horizons. Hayward was able to use this quasi-local construct to arrive at the first and second law of black hole mechanics elegantly without any the underlying problems of using a global teleological construct. A discussion of how Hayward does this is provided in Chapter (6). The surface at where the requirements above hold can be found for some spherically symmetric metric expressed generally in Painleve-Gullstrand coordinates as [49]:

$$ds^2 = -e^{-2\Phi(\tau,r)}(1 - \frac{2m(t,r)}{r})d\tau^2 + 2e^{-\Phi(\tau,r)}\sqrt{\frac{2m(\tau,r)}{r}}d\tau dr + dr^2 + r^2 d\Omega^2. \tag{5.5}$$

For the case of radial null geodesics, $ds = d\Omega = 0$, thus giving:

$$\frac{dr}{d\tau} = -e^{-\Phi(\tau,r)}(1 \pm \sqrt{\frac{2m(\tau,r)}{r}}). \tag{5.6}$$

The outgoing null geodesics is therefore, expressed as:

$$l^a = (e^{\Phi(\tau,r)}, 1 - \sqrt{\frac{2m(\tau,r)}{r}}, 0, 0). \tag{5.7}$$

Similarly for ingoing null geodesics:

$$n^a = \frac{1}{2}(e^{\Phi(\tau,r)}, -1 - \sqrt{\frac{2m(\tau,r)}{r}}, 0, 0). \tag{5.8}$$

The factor of a $\frac{1}{2}$ ensures that the normalisation requirement $n^a l_a = -1$. Thus the expansion of these geodesics can be computed using Eq (5.2) to give:

$$\theta_l = \frac{2}{r}(1 - \sqrt{\frac{2m(\tau,r)}{r}}). \tag{5.9}$$

And for the ingoing geodesics:

$$\theta_n = -\frac{1}{r}(1 + \sqrt{\frac{2m(\tau, r)}{r}}). \tag{5.10}$$

Ergo, θ_n is always negative, whilst $\theta_l = 0$ at the surface $r = 2m(\tau, r)$. Also, Eq (5.2) can be analysed to ascertain the nature of an outer horizon at $r = 2m$. Computing $n^a \nabla_a \theta_l$ at the horizon H at $r = 2m$:

$$(n^a \nabla_a \theta_l)_H = -\frac{(1 - 2m'_H)}{r_H^2}(1 + \frac{\dot{r}_H}{2e^{-\Phi_H}}). \tag{5.11}$$

Where $m'_H = \frac{\partial m_H}{\partial r}$ and $\dot{r}_H = \frac{\partial r_H}{\partial \tau}$. This is negative when $2m'_H < 1$. Also at $r = 2m$, $\dot{r}_H = -2e^{\Phi_H}$. So we have an outer horizon at $r = 2m$ if $2m'_H < 1$ and the horizon is not moving inwards faster than ingoing null geodesics. To ascertain what type of hypersurface occurs at $r = 2m$, we must find the norm of the normals to the surface in question. If the normal to the surface at $r = 2m$ is denoted by N^a, then the norm is given by:

$$N^a N_a = -4\dot{m}e^{2\Phi} - -4\dot{m}e^{\Phi}(1 - 2m'). \tag{5.12}$$

In the static case where $\dot{m} = 0$, the trapping horizon is a null hypersurface. If the mass is increasing as a function of time, $\dot{m} > 0$, then it is a spacelike hypersurface for $1 - 2m' > 0$. Conversely, if the mass is decreasing, $\dot{m} < 0$ and $-(1 - 2m')e^{\Phi} < \dot{m}$ then a timelike hypersurface is described. This of course has important consequences for our understanding of these trapping horizons as it raises the possibility to travel along a causal curve inside an evaporating black hole and end up outside the trapping horizon region. In dynamical cases, the event horizon is not defined by the surface $r = 2m$. The event horizon, is by definition, always a null hypersurface and only coincides with the trapping horizon if the spacetime is globally static.

5.3 Dynamical Horizons

One can take the trapping horizon considerations but apply them to dynamic spacetimes, where there is a matter flux across the horizon surface. This led Ashtekar and Krishnan to define the *dynamical horizon* (DH). The DH is essentially a spacelike FOTH that satisfies $n^a \nabla_a \theta_l < 0$

A smooth, three dimensional spacelike, submanifold, S, that can be foliated by a family of closed 2-surfaces so that [25]:

1. On each leaf, $\theta_{(l)} = 0$
2. $\theta(n) < 0$

Ashtekar and Krishnan used DH to construct area increase laws and generalised laws of black hole mechanics without the condition that governs the sign of $n^a \nabla_a \theta_l < 0$.

It is advantageous to construct the DH as such as by definition it only refers to the intrinsic geometry of S.

FOTH and DH are not defined using future infinities as is the case in event horizons and they are truly quasi-local constructs that do not permit teleological properties.

5.4 Isolated Horizons

Ashtekar and Krishnan similarly laid out the foundation for *isolated horizons* (IH). These horizons model black holes in equilibrium. The spacetime surrounding the black hole that permits an IH may be dynamical, but the the black hole itself is in equilibrium. The key in defining IH is in generalising notions of the Killing horizon by attempting to find minimal conditions that allow useful physics to be defined (mass, angular momentum etc). IH are three dimensional sub-manifolds of spacetime like the DH, but unlike the DH, they are null (just as Killing horizons are). We will discuss mostly in this section about *weakly* isolated horizons (WIH), as they are suitable for most intents and purposes. A three-surface can only be a WIH if it is a non-expanding horizon (NEH). We can define the an NEH as follows:

A submanifold, H, of a spacetime is a NEH if:

1. It is null.
2. $\theta_{(l)} = 0$, I.e. vanishing expansion of null normal to H.
3. $-T^b_a l^a$ is future directed and causal.
4. All field equations hold on H.

This submanifold is also a WIH if its full geometry is not evolving along null generators. So that for the null normals:

$$(\mathcal{L}_l \mathcal{D}_a - \mathcal{D}_a \mathcal{L}_l) l^b = 0. \tag{5.13}$$

Where $\mathcal{D}$ is a derivative operator on H. The nature of this derivative operator is found by considering the intrinsic geometric properties of the NEH [50]. The spacetime derivative operator ∇_a induces $\mathcal{D}$ on H. To strengthen this notion, the differential operator $\mathcal{D}$ must be time independent and apply to all tangential vectors V^a to H. Ergo, Eq (5.13) becomes:

$$(\mathcal{L}_l \mathcal{D}_a - \mathcal{D}_a \mathcal{L}_l) V^b = 0. \tag{5.14}$$

Looking back at the WIH, if one is to foliate H into two surfaces, the null condition on the surface along with the requirement $\theta_{(l)} = 0$ ensures, that for the area form of the horizon $\mathcal{A}$, $\mathcal{L}_l \mathcal{A} = 0$. This implies that l^a is a Killing vector on H and that H itself is a Killing horizon. We have not imposed any conditions on the spacetime surrounding H, only on H itself. Thus, the spacetime surrounding H can be dynamic and H can still be a WIH or IH.

5.5 Conformal Killing Horizons

The laws of black hole thermodynamics depend explicitly on the area of of the black hole, as outlined in the previous section. However, as the area of the black hole remains a contested feature, there is some confusion that quite naturally arises when one mentions these laws: If Hawking-Bekenstein entropy is indeed a real measurable quantity then there should be a real, measurable area. In static, stationary spacetimes the event horizon simply coincides with the Killing horizon, thus making the task of measuring thermodynamic properties associated with black holes relatively easy. However, this is certainly not the case for dynamical spacetimes. In fact, the correct way to calculate thermodynamic properties in dynamical black hole spacetimes remains an open question [11]. But there are some mathematical techniques one can use to gain valuable insight into the matter, one such technique is *conformal* transformations. In the context of General relativity, a conformal transformation takes a special class of dynamical spacetimes and maps them to a static spacetime. It is then of interest to note that if this spacetime permits a Killing vector, then there exists a conformal Killing horizon which is a null surface in the dynamical spacetime. Such spacetimes, that permit conformal Killing horizons are of particular interest as they provide a mathematical technique to analyse phenomena associated with dynamical spacetimes in a corresponding static spacetime. The previously mentioned quasi-local horizons all rely on marginal trapped surfaces. As the conformal Killing horizon must always be a null surface, it cannot coincide with the dynamical horizon which is by definition always spacelike.

We have seen before, that a Killing vector must obey the Killing vector field equation:

$$\nabla_a \chi_b + \nabla_b \chi_a = 0. \tag{5.15}$$

The Killing horizon is a null hypersurface where χ^a is orthogonal to it at all point. On the Killing horizon, this orthogonality condition can be expressed in the Frobenius form as:

$$\chi_{[a} \nabla_b \chi_{c]} = 0. \tag{5.16}$$

On our Lorentzian manifold $(\mathscr{M}, g_{ab})$. One can perform a conformal transformation on the metric g_{ab} thus:

$$\bar{g}_{ab} = \Omega^2 g_{ab} \tag{5.17}$$

$$\bar{g}^{ab} = \Omega^{-2} g^{ab} \tag{5.18}$$

$$\Omega \neq 0. \tag{5.19}$$

Where Ω^2 is a smooth function on the manifold $\mathscr{M}$, called the conformal factor.

One can also find the conformal Killing Horizon, which is defined similarly to the regular Killing Horizon. The Conformal Killing Horizon is some null hypersurface

$\bar{\Sigma}$ which is a smooth codimension one embedded submanifold of $\mathscr{M}$ which has an orthogonal Killing vector χ^a. It satisfies the conformal Killing equation:

$$\nabla_\mu \chi_\nu + \nabla_\nu \chi_\mu = 2\Omega^2 g_{ab}. \tag{5.20}$$

5.5.1 In the Linear Vaidya Spacetime

The Vaidya metric can briefly be understood as s simple dynamical spacetime. It describes the spacetime resulting from a spherically symmetric, non-rotating body that emits or absorbs null dust.

In conformally static in-going Vaidya spacetime, the metric in Eddington-Finkelstein coordinates is: [22]:

$$ds^2 = -(1 - \frac{2M(v)}{r})dv^2 + 2dvdr + r^2 d\Omega^2. \tag{5.21}$$

Where $M(v)$ can be any function of v and the resulting spacetime is an exact solution which is consistent with the Einstein equations for null dust [11]. Assuming $M(v)$ takes a linear form, we can find conformal factors that permit such a mapping:

$$M(v) = M_0 + \alpha(v - v_0). \tag{5.22}$$

M_0 and v_0 are constants and $\alpha = \frac{dM}{dv}$. This permits conformal Killing equations that satisfy the conformal Killing equation, Eq (5.20) for the conformal Killing vector field:

$$\chi^a = \frac{M(v)}{M}\delta^a_v + \frac{\alpha r}{M}\delta^a_r. \tag{5.23}$$

This is null for $\chi^a \chi_a = 0$:

$$\chi^a \chi_a = \frac{M(v)}{M^2}[2\alpha r - M(v)(1 - \frac{2M(v)}{r})] = 0. \tag{5.24}$$

Which has solutions when:

$$r = \frac{M(v)}{4\alpha}(1 \pm \sqrt{1 - 16\alpha}). \tag{5.25}$$

It is found in [11] that the conformal factor that allows a transformation from linear Vaidya to static spacetimes is:

$$\Omega^2 = \frac{M(v)r}{2M_0^2}. \tag{5.26}$$

6 BLACK HOLE MECHANICS IN QUASI-LOCAL HORIZONS

This section explores ways in which black hole thermodynamics has been formulated for quasi-local horizons. The fact that black hole mechanics can be derived via alternative formulations of the horizon region further supports the notion that the event horizon as defined by Hawking and Ellis [4] is incredibly limited in that the laws of black hole mechanics outlined in [1] are done so for stationary black holes where the event horizon coincides with a Killing horizons. Coupled with the event horizon's limitations in Chapter (3), it is apparent that the event horizon may just be an unsuitable theoretical construct to describe the black hole region.

6.1 Black Hole Thermodynamics via Hayward and Trapping Horizons

Hayward was able to show that the laws of black hole thermodynamics can be arrived at from quasi-local notions in spacetime in an elegant and precise manner [48]. He developed the notion of a Future Outer Trapping Surface and was able to show that this spatial construct, quasi-local and not permitting any teleological properties can be used to find the zeroth, first and second laws of black hole thermodynamics.

6.1.1 Zeroth and First Law for Trapping Horizons

The zeroth law of black hole mechanics, as we have seen, is summarised simply as the surface gravity κ being constant over the horizon surface. To begin formulating analogous laws of black hole mechanics for the trapping horizon, it is imperative to construct a working analogous definition for the surface gravity κ. It is initially noted that surface gravity is only formulated using Killing horizons for the case of stationary black holes. Hayward argues that due to the event horizon's global structure it can not have a quasi-local definition of surface gravity. It is relatively straightforward to derive the laws of black hole mechanics from the notion of trapping horizons. To begin formulating black hole mechanics for the trapping horizon, consider the surface defined by the trapping horizon: $r = 2m(\tau, r)$, which can be differentiated with respect to some parameter λ to give:

$$\frac{dr}{d\lambda} = 2\frac{\partial m}{\partial \tau}\frac{d\tau}{d\lambda} + 2\frac{\partial m}{\partial r}\frac{dr}{d\lambda}. \tag{6.1}$$

If the area of the horizon surface is simply given as $A = 4\pi r^2$, and $\lambda = \tau$. Then Eq(6.1), after some rearranging becomes:

$$\frac{\partial m}{\partial \tau} = \frac{1}{8\pi}\frac{(1-2m')}{2r}\frac{dA}{d\tau}. \tag{6.2}$$

This appears strikingly similar to the first law: $dM = \frac{1}{8\pi}\kappa dA$, as such it seems appropriate to take the surface gravity to be $\kappa = \frac{(1-2m')}{2r_H}$[49].

6.1.2 Second Law for Trapping Horizon

In order to arrive at the second law, simply compute $G_{ab}l^a l^b$, where G_{ab} is the Einstein tensor. For the spherically symmetric metric defined by Eq (5.5), this is simply found to be:

$$G_{ab}l^a l^b = \frac{2e^{\Phi}}{r^2}\frac{\partial m}{\partial \tau}\sqrt{\frac{2m}{r}} - \frac{2}{r}\frac{\partial \Phi}{\partial r}(1-\sqrt{\frac{2m}{r}})^2. \tag{6.3}$$

Rearranging:

$$\frac{\partial m}{\partial \tau} = \frac{1}{2}e^{-\Phi}r^2\sqrt{\frac{2m}{r}}G_{ab}l^a l^b + e^{-\Phi}\frac{\partial \Phi}{\partial r}r\sqrt{\frac{r}{2m}}(1-\sqrt{\frac{2m}{r}})^2. \tag{6.4}$$

Using the result found in Eq (6.2), the area law can be expressed:

$$\frac{\partial A}{\partial \tau} = \frac{16\pi r^3 e^{-\Phi}}{1-2m'}G_{ab}l^a l^b. \tag{6.5}$$

$G_{ab} \propto T_{ab}$, ergo if $T_{ab}l^a l^b > 0$ so that the null energy condition is satisfied, then the area is always increasing.

6.2 Black Hole Mechanics for Isolated Horizons

6.2.1 Zeroth law for Isolated Horizons

The zeroth law for isolated horizons arises very naturally in an analogous manner as for Killing horizons. Null normal vectors l^a to the isolated horizons must generate a congruence of null geodesics, which in the same manner as in [1], must have some function κ_I such that:

$$l^a \nabla_a l^b = \kappa_I l^b. \tag{6.6}$$

κ_I is interpreted as the surface gravity on the isolated horizon. So each choice of l^a will generate a κ_I on the isolated horizon surface.

6.2.2 First Law for Isolated Horizons

The first law for isolated horizons arises by considering Hamiltonians in spacetimes with an isolated horizon as its boundary. One must define what the mass is in spacetimes that permit isolated horizons and whether an action principle can be formulated for such a case. As usual, the Hamiltonian formulated in [51] contains both bulk and boundary terms. Bulk terms will be zero for any solution to the Einstein equation. The remaining boundary terms are interpreted as the energies associated with the isolated horizon.

Formulating the first law requires one to find angular momentum and energy of the isolated horizon region. As we are employing a Hamiltonian strategy, one must consider

some covariant phase space, Γ that has a symplectic structure, ω. A symplectic structure is one which is a closed non-degenerate 2-form. Considering infinitesimal variations on Γ, δ_1 and δ_2, the action of these variations $\omega(\delta_1, \delta_2)$ provides a function on Γ. If some vector field V on Γ satisfies the requirement $\mathcal{L}_A\omega = 0$, then it is Hamiltonian. Furthermore, this condition applies if for some function H on Γ: $\omega(\delta, V) = \delta H$ for all vector fields. Then one can assign H as the Hamiltonian and V, the Hamiltonian vector field. In other words, H generates the infinitesimal canonical transformations V. These infinitesimal canonical transformations correspond to time translations and rotations. In this formalism, the Hamiltonian provides bulk terms which provide ADM formulas for mass and energy, and the boundary terms which one would expect to coincide with energy and angular momentum on the isolated horizon.

Considering, the horizon's angular momentum first, the resulting expression found contains two terms: a term that represents the angular momentum at the isolated horizon, and the other term that gives variation of ADM angular momentum. To find an appropriate expression, one must consider some boundary conditions for a vector field ϕ^a on our spacetime:

1. Approaching infinity, ϕ^a is simply associated with fixed rotational symmetry of Minkowski spacetime.
2. On the isolated horizon, it coincides with the rotational vector ζ^a. This rotational vector ensures that the WIH is geometrically a Ashtekar 'type II' isolated horizon which ensures axi-symmetry.

One now must find the function J which in this formalism satisfies $\delta J = \omega(\delta, V_{(\phi)})$, for any variation δ. Carrying out the direct calculation as found in [52] one finds:

$$\delta J = -\frac{1}{8\pi}\delta \oint_S [(\zeta^a \eta_a)^2 \mathcal{A}] - \delta J_{ADM}. \tag{6.7}$$

Where S is the cross section across which we are evaluating the integral. η_a is a one form on the isolated horizon that obeys: $X^a \nabla_a l^b = X^a \eta_a l^b$ for any vector tangential to the isolated horizon, X^a. It is related to κ via $\kappa_I = l^a \eta_a$. The surface integral is interpreted as the variation in the angular momentum at the isolated horizon, δJ_I. One therefore, simply finds:

$$J_I = -\frac{1}{8\pi} \oint_S (\zeta^a \eta_a)^2 \mathcal{A}. \tag{6.8}$$

This expression is completely dependent on the local geometry on the type II horizon.

For the horizon energy, one must find the Hamiltonian along a time translation symmetry, t^a, on the spacetime. t^a on the isolated horizon surface is a linear combination of the null normal, l^a, and axial symmetry vector ϕ^a :

$$t^a = B_{(l,t)} l^a - \Omega_{(t)} \phi^a. \tag{6.9}$$

Where $B_{(l,t)}$ and $\Omega_{(t)}$ are constants on the isolated horizon surface but differ on different spacetimes. Once again the strategy is essentially the same. Evaluating the action of the one form $T_{(t)}$ on a tangential vector field δ:

$$T_{(t)}(\delta) = \omega(\delta, V_{(t)}). \tag{6.10}$$

Once again, evaluating Eq (6.10) yields a ADM term coinciding with the surface term at infinity and a surface term at the isolated horizon. Ashtekar and Krishnan find this to be:

$$T_{(t)}(\delta) = -\frac{\kappa_I}{8\pi}\delta a_I - \Omega_{(t)}\delta J_I + \delta E_{ADM}. \tag{6.11}$$

$\kappa_I = B_{(l,t)}l^a\eta_a$, a_I is the area of the isolated horizon and E_{ADM} is the ADM energy associated with the time translation symmetry. The first two terms in Eq (6.11) are associated with the energy of the isolated horizon. Thus, Eq (6.11) is Hamiltonian if there is some a function, E_I on Γ satisfying:

$$\delta E_I = \frac{\kappa_I}{8\pi}\delta a_I + \Omega_{(t)}\delta J_I. \tag{6.12}$$

E_I thus represents the energy on the isolated horizon. This is analogous to the standard first law for black hole mechanics.

6.3 Black Hole Mechanics for Dynamical Horizons

6.3.1 Second law for Dynamic Horizons.

Before talking about the first law for dynamic horizons, it perhaps makes more sense to discuss the area increase law for dynamic horizons first. Part of the reason as to why quasi-local horizons are considered so important by many is due to the need for generalised laws of black hole mechanics that work in dynamic spacetimes. Naturally, a more physical form of the area increase law would take into account local matter-energy fluxes across the horizon. Ashtekar and Krishnan do this by providing area balance laws for dynamic horizons to show how they respond to matter-energy fluxes across the horizon. The area balance law that arises from considering how local geometric structures are affected by the flux of matter and energy across the dynamic horizon via Ashtekar and Krishnan are:

$$\frac{R_2}{2} - \frac{R_1}{2} = \int_S N_R T_{ab}\hat{\tau}^a l^b d^3V + \frac{1}{16\pi}\int_S N_R(\hat{\sigma}_{ab}\hat{\sigma}^{ab} + 2\zeta^a\zeta_b)d^3V. \tag{6.13}$$

r_1 and r_2 are simply the areal radii of different foliations of the dynamic horizon. $\hat{\tau}^a$ is simply the unit timelike normal to the foliation, chosen such that $g_{ab}\hat{\tau}^a\hat{\tau}^b = -1$. N_r is a lapse function such that $N_R = |\partial R|$. R is the area-radius increase function which is constant on each foliation and satisfies $a = 4\pi R^2$. Where a is the area of the respective foliation. It was shown in [25] that this area increases monotonically, hence R is an appropriate choice on the dynamic horizon. $\zeta^a = \hat{q}^{ab}\hat{r}^c\nabla_c l_b$, where $\hat{q}_{ab}$ is the

intrinsic metric such that $\hat{q}_{ab} = g_{ab} + \hat{\tau}_a\hat{\tau}_b$. $\hat{r}^a$ is the unit spacelike normal to some foliation of the dynamic horizon.

Although the direct physical consequence is not immediately obvious, Eq (6.13) can be simply interpreted as the sum of the matter-energy flux across the dynamic horizon. The left hand side of Eq (6.13) is simply the change in the horizon radius due to the dynamical process. The first integral on the right hand side is interpreted as the flux associated with matter-energy, $\mathcal{F}_m$ whilst the second integral on the right is associated with the flux due to gravitational radiation, $\mathcal{F}_g$. Ergo, Eq (6.13) can be interpreted as:

$$\frac{1}{8\pi}(\frac{A_2}{R_2} - \frac{A_1}{R_1}) = \mathcal{F}_m + \mathcal{F}_g. \tag{6.14}$$

6.3.2 First law for Dynamic Horizons

A more detailed analysis of the area increase law for dynamic horizons tells us that the law was derived for the Hawking mass which is interpreted as the mass of the horizon. This is adequate in the case of a spherically symmetric spacetime, however in more general spacetimes, such as Kerr, this interpretation does not hold. Therefore, a more general expression needs to be found. Employing a similar strategy as for the WIH whereby a suitable linear combinations of l^a and ϕ^a were chosen, we can find a time translation symmetry on the dynamic horizon that has time dependent coefficients. A deeper dive into Ashtekar and Krishnan's area increase law for dynamic horizons reveals that they found the matter-energy flux associated with the vector fields $\xi^a = Nl^a = N\hat{\tau}^a + N\hat{r}^a$.

The time translation symmetry used by Ashtekar and Krishnan to generalise the area increase law is of the form:

$$t^a = N_r l^a + \Omega\phi^a = N_r\hat{\tau}^a + (N_r\hat{r}^a + \Omega\phi^a). \tag{6.15}$$

The lapse function N_r is given by $N_r = |\partial r|$ for any function r of R. Ω is an arbitrary function of R. The generalised form of Eq (6.13) becomes:

$$\mathcal{F}^t = \frac{R_2}{2} - \frac{R_1}{2} + \frac{1}{8\pi}(\oint_{S_2} \Omega j^\phi d^2V - \oint_{S_1} \Omega j^\phi d^2V - \int_{\Omega_1}^{\Omega_2} d\Omega \oint_S j^\phi d^2V). \tag{6.16}$$

Where $j^\phi = -K_{ab}\phi^a\hat{r}^b$. K_{ab} is the extrinsic curvature of the dynamic horizon. j^ϕ is defined as the angular momentum density. S_1 and S_2 refer to cross sections of the dynamic horizon region. If these cross sections are only infinitesimally separated then Eq (6.16) reduces to:

$$\delta M = \frac{1}{8\pi}(\frac{1}{2R}\frac{dr}{dR})|_S\delta a + \Omega\delta J. \tag{6.17}$$

It appears natural to take $\kappa = (\frac{1}{2R}\frac{dr}{dR})$ to be the effective surface gravity on some cross section S.

6.4 Black Hole Mechanics for Conformal Killing Horizons

Conformal Killing horizons in linear Vaidya spacetimes can also be used to construct laws of black hole mechanics quasi-locally. This discussion largely follows work that can be found in [11].

6.4.1 Zeroth Law for Conformal Killing Horizons

The change in mass function along the horizon direction in [11] is found to be:

$$\mathcal{L}_\chi m = \frac{\alpha M(v)}{M_0}. \tag{6.18}$$

Whilst the change in horizon area is:

$$\mathcal{L}_\chi A = \frac{2\alpha A}{M_0}. \tag{6.19}$$

The mass function can be interpreted as the energy on the horizon, whilst the area is related to the entropy of the black hole via the Hawking-Bekenstein relation: $S = \frac{1}{4}A$. Therefore, one can consider the thermodynamics associated with the conformal killing horizon by calculating the effective temperature T_{eff}:

$$T_{eff} = \frac{\mathcal{L}_\chi M}{\mathcal{L}_\chi S} = \frac{4\mathcal{L}_\chi m}{\mathcal{L}_\chi A} = \frac{4\alpha^2}{\pi M(v)(1 - 8\alpha - \sqrt{1 - 16\alpha})}. \tag{6.20}$$

In the case of a Schwarzschild black hole (static case), $\alpha \to 0$. This leads Eq(6.20) to reduce to the expected temperature of a Schwarzschild black hole: $T = \frac{1}{8\pi M}$.

In a similar way to the laws of black hole mechanics, the surface gravity κ_C on the conformal Killing horizon can be found by the relation: $\nabla_a(\chi^a\chi_a) = -2\kappa_C\chi_a$. Using this relation, κ_C is found to be:

$$\kappa_C = \frac{2\alpha\sqrt{1 - 16\alpha}}{M_0(1 - \sqrt{1 - 16\alpha})}. \tag{6.21}$$

This value is constant across the conformal Killing horizon, thus satisfying the zeroth law of black hole mechanics. In the static limit, $\alpha \to 0$, this takes the expected Schwarzschild value of $1/4M$. Nielsen and Shoom argue that to obtain measurable temperature in the static limit, the conformal Killing vector, given by Eq (5.23), must be normalised to coincide with the four-velocity of the observer at their location, via the relation:

$$\chi^a \to \tilde{\chi}^a = \gamma\chi^a. \tag{6.22}$$

Where γ is some constant Nielsen and Shoom find γ to be:

$$\gamma = \frac{1}{\sqrt{\frac{2M(v)}{r}(1 - \frac{2M(v)}{r}) - 4\alpha)}}. \tag{6.23}$$

For a trajectory along the conformal Killing vector in the Vaidya spacetime, the surface gravity is given by $\kappa = \Omega\gamma\kappa_C$. This is because the static spacetime is required to have the same physics as in the linear Vaidya spacetime, κ is thus found to be:

$$\kappa = \frac{r^{1/2}}{\sqrt{M^2 r - 2M^3 - 2\alpha M r^2}} \frac{2\alpha\sqrt{1-16\alpha}}{(1-\sqrt{1-16\alpha})}. \tag{6.24}$$

Eq (6.24) is evaluated at the observer's location.

6.5 Discussion

We have seen in this section a brief review of the various ways in which quasi-local horizons have been used to formulate the laws of black hole mechanics, which are some of the most celebrated results in the history of black hole physics. It is clear that whilst the event horizon has been useful in the development of our understanding of black hole and intuitively grasping the expected behaviour of black holes, the event horizon should perhaps not be taken as gospel. While there is little agreement as to which quasi-local horizon is the best match for the black hole region, many theoreticians appear to agree that the event horizon is not suitable for a full description of a black hole [48][34] [5][25][6][53]. For those who wish to understand the black hole region in a more physical way without global or teleological problems, quasi-local horizons would appear to be stronger candidates.

7 RINDLER HORIZONS

In this section we look at Rindler horizons that form in flat, Schwarzschild and Vaidya spacetimes, respectively. We extend the work done by Paithankar and Kolekar [54] [55] to a dynamical black hole spacetime (modelled by the Vaidya solution) and numerically reproduce some of their key results in Eddington-Finkelstein coordinates. We construct these numerical simulations to explore the thermodynamic links between null quasi-local black hole horizons and Rindler horizons.

7.1 Rindler Trajectories and Their Horizons

Rindler trajectories are a class of trajectories often considered in flat spacetime. In flat Minkowski spacetime, a uniformly accelerating particle experiences hyperbolic motion. The region of spacetime containing Rindler trajectories, is constrained on the $T = X$ and $T = -X$ part of the Minkowski diagram, this area forms the Rindler chart [38]. Figure (7.1) shows the Rindler chart plotted in Minkowskian coordinates.

Rindler trajectories can be used to describe the Unruh effect whereby linear uniformly accelerated observers will measure an effective temperature associated with their acceleration in a vacuum field [9]. This surprising result is somewhat analogous to the expected Hawking radiation in a black hole region. The Unruh effect arises from considering the vacuum of quantum fields in Minkowski spacetime for some constant uniformly accelerating frame. A thermal effect is then expected for some observer. If we consider this special case of hyperbolic motion in Minkowski spacetime with some constant magnitude of acceleration $|a|$, then Unruh shows that this leads to a notion of temperature defined at the Rindler horizon. This temperature, T_u, is given by $|a|/2\pi$. The tantalising link between Rindler horizons and thermodynamics has also been explored in [56], where the generalised second law is proved for rapidly evolving semi-classical Rindler horizons. This work was further extended to prove the generalised second law for all causal null horizons (which includes the Rindler horizon)[10]. Many of the quasi-local horizons we have discussed are not null. The dynamical horizon, for example is spacelike. Trapping horizons, as we have seen can be spacelike or timelike. A quasi-local black hole horizon that is null and therefore can obey the generalised second law, is the conformal Killing horizon. This link between causal null horizons and the generalised second law motivates a study of to what extent (if any) the Rindler horizons share thermodynamic properties with the conformal Killing horizons.

Rindler trajectories have been used to describe motion in the case of a static spherically symmetric black hole a large distance from the Rindler observer. [54] [55]. There is potential to use a class of observers permitting Rindler horizons in a black hole spacetime to also find conformal Killing horizons therefore associating

a thermodynamic process that arises at Rindler horizons, the Unruh effect, with a quasi-local horizon. This chapter attempts to build on the work in [54] and [55] to find generalised Rindler trajectories in the Schwarzschild and Vaidya spacetimes. The Rindler horizons that we will look at are spherically symmetric for a spherical shell of observers accelerating outwards in every direction and not just simply for a single observer.

The Vaidya spacetime is of special importance here as it permits conformal Killing horizons for certain spacetimes (the linear Vaidya, for example). Therefore, one can in principle find a Rindler horizon in a background Vaidya spacetime that also permits a conformal Killing horizon and compare their differences. Also, the conformal Killing horizon may be associated with the Unruh temperature for certain black hole spacetimes. In flat Minkowski spacetimes the Rindler horizon is a Killing horizon, ergo the Killing horizon in this scenario has a thermodynamic property naturally associated with it via the Unruh effect. By extension, if the conformal Killing horizon, has temperature, it must have some associated entropy which can be compared with results found in [11]. This section will mostly deal with numerically finding such Rindler horizons in black hole spacetimes.

In a spacetime that contains a black hole, the geometry is still mostly flat for observers a large distance away from the black hole, however there will be small perturbations due to the black hole region [54]. We shall consider in this chapter, a full family of radially accelerated observers in various black hole spacetimes that are set to begin at some radial distance of closest approach r_{min} and accelerate away from the black hole region with constant magnitude of proper acceleration $|a|$. We shall consider similar constraints to [54], i.e. constant magnitude of acceleration as well as a further constraint such that the trajectory must be linear with vanishing *torsion* and *hyper-torsion*. In [38] such a constraint is found for a general curved background spacetime:

$$\mu^j \nabla_j a^i - |a|^2 \mu^i = 0. \tag{7.1}$$

Where μ^i is the four-velocity of the LUA observer. This constraint was found by generalising the Minkowskian rectangular hyperbola's differential geometric properties to a general curved background spacetime. The consistent solution to Eq (7.1) is given by the required trajectory of the LUA observer. This constraint was also derived in [57] by finding the only non-trivial Letaw-Frenet equation.

7.2 Rindler Trajectories in Flat Spacetime

We will briefly discuss the common approach to Rindler trajectories in flat spacetime by considering constantly accelerating hyperbolic motion in the usual Minkowski spacetime.

Assuming a flat Minkowski, spacetime with the line element:

$$ds^2 = -dT^2 + dX^2 + dY^2 + dZ^2. \tag{7.2}$$

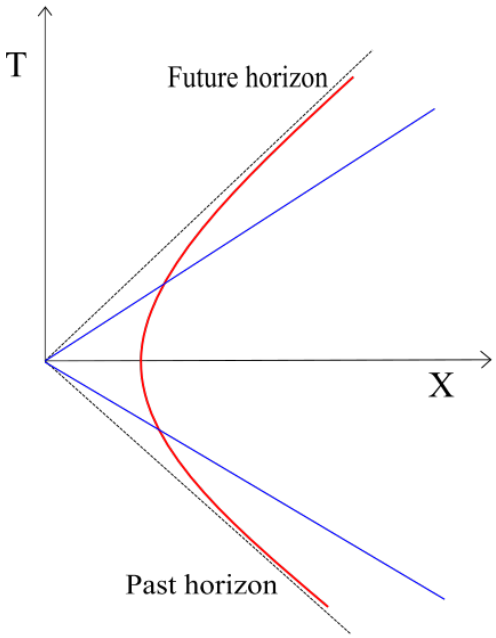

Figure 7.1: Figure showing the right hand side of the *Rindler wedge*. Dashed lines show the Rindler horizons. The blue lines show lines of some constant t with red lines showing the lines of some constant x. The red line is the worldline of an accelerating observer for whom the dotted 'future horizon' acts as the Rindler horizon.

One can transform to hyperbolic coordinates to obtain a Minkowski line element for the Rindler chart. Letting a be the proper acceleration, then:

$$T = xsinh(at) \qquad X = xcosh(at) \qquad Y = y \qquad Z = z.$$

Performing the transformation, the Minkowski line element for the Rindler chart

becomes [57]:

$$ds^2 = -a^2x^2dt^2 + dx^2 + dy^2 + dz^2. \tag{7.3}$$

In flat Minkowski spacetime, the Rindler trajectories are confined to the Rindler quadrant, the right hand wedge of the Minkowski spacetime, bounded by $X = T$ and $X = -T$. The Rindler coordinates are specially adapted to the Rindler trajectory such that x and t are fixed along the LUA trajectory.

One may now ask the question of what might happen in non-flat, non-trivial spacetimes? I.e. spacetimes that have curvature due to some astrophysical object, a black hole, say? This requires a generalisation of the Rindler trajectory to account for curvature. The constraint which allows us to generalise the Rindler trajectory to a more general linear uniformly accelerating (LUA) trajectory is given by Eq (7.1).

7.3 LUA Trajectories in Schwarzschild Spacetime

For the Schwarzschild metric in in-going Eddington-Finkelstein coordinates:

$$ds^2 = -(1 - \frac{2M}{r})dv^2 + 2dvdr + r^2d\Omega^2. \tag{7.4}$$

One can extract LUA trajectories in spherical symmetry, where the 4-velocity is of the form: $\mu^i = (A(v,r), B(v,r), 0, 0)$. μ^i is parameterised by proper time, thus $\mu^i\mu_i = -1$. This gives a relation between $A(v,r)$ and $B(v,r)$:

$$B = \frac{1 - \Delta A^2}{2A}. \tag{7.5}$$

Where $\Delta = (1 - \frac{2M}{r})$. The equation of motion is obtained from $\frac{dr}{dv} = \frac{B}{A}$:

$$\frac{dr}{dv} = \frac{1 - \Delta A^2}{2A^2}. \tag{7.6}$$

Therefore, solving for A will give the equation of motion which also provides the required LUA trajectory in a background Schwarzschild spacetime to find the Rindler Horizons as the LUA trajectory accelerates away from the black hole region. To calculate the components of 4-acceleration, use $a^i = \mu^j\nabla_j\mu^i$:

$$a^0 = \frac{dA}{d\tau} + \frac{M}{r^2}A^2 \tag{7.7}$$

$$a^1 = \frac{dB}{d\tau} + \frac{2M\Delta}{r^2}A^2 - \frac{M}{r^2} \tag{7.8}$$

$$a^3 = a^4 = 0. \tag{7.9}$$

Using the constraint equation $\mu^j\nabla_j a^i - |a|^2\mu^i = 0$ [54] and assuming the magnitude of proper acceleration is constant, we arrive at the following second order non-linear ordinary differential equation from the time component:

$$\frac{da^0}{d\tau} + \frac{M}{r^2}Aa^0 - |a|^2 A = 0. \tag{7.10}$$

Similarly for the radial component:

$$\frac{da^1}{d\tau} + \frac{M\Delta}{r^2}Aa^0 - \frac{M}{r^2}Aa^1 - \frac{M}{r^2}Ba^0 - |a|^2 B = 0. \tag{7.11}$$

Eq (7.10) expressed fully in terms of A becomes:

$$\frac{d^2A}{d\tau^2} + \frac{3M}{r^2}A\frac{dA}{d\tau} + \frac{M(r-M)}{r^4}A^3 - (\frac{M}{r^3} + |a|^2)A = 0. \tag{7.12}$$

7.3.1 Acceleration Bounds in Schwarzschild Spacetime

Returning to the Schwarzschild case one expects a LUA trajectory $\mu^i \to (1,1,0,0)$, which coincides with some radial null ray. As A_0, the initial value of A, is > 1 at r_{min}, this requires $\frac{dA}{d\tau} < 0$, whist $\frac{d^2A}{d\tau^2} > 0$. One can therefore find bounds on the values of $\frac{dA_0}{d\tau}$ by considering these requirements and applying them to Eq (7.12) for $r = r_{min}$. In general for any r throughout the trajectory:

$$\frac{dA}{d\tau} > \frac{r^2}{3M}[(\frac{M}{r^3} + |a|^2 - \frac{M}{r^4}(r-M)A^2]. \tag{7.13}$$

Eq (7.13) at $r_{min} = 3M$, for example becomes:

$$\frac{dA}{d\tau} > 3M(|a|^2 - \frac{1}{27M^2}). \tag{7.14}$$

Thus if $M = 1$:

$$3(|a|^2 - \frac{1}{27}) < \frac{dA}{d\tau} < 0. \tag{7.15}$$

So in this example, a bound is found for the magnitude of the 4-acceleration in Schwarzschild spacetime that permits a LUA trajectory if the distance of closest approach to the black hole is $3M$:

$$|a| < \frac{\sqrt{3}}{9}. \tag{7.16}$$

This is in agreement with the bound found in [54].

7.4 LUA Trajectories in Vaidya Spacetime

LUA trajectories in background Schwarzschild spacetimes have already been discussed in the literature [54] [55]. However, there are some key limitations to the Schwarzschild solution which motivates the need to generalise LUA trajectories to black holes which are a more accurate representation of physical reality. One can understand this requirement by simply considering a summary of the common model of stellar collapse to form a stellar black hole and the evolution of black holes. Initially, a very large star approaching the end of its lifespan will begin to collapse due to gravity under its own mass and then eventually 'blows apart' in a supernovae. The irreversible collapse of the core will also trigger the formation of a stellar mass black hole. These stellar mass black holes form with a lot of mass accreted in a very short time, They eventually reach a more 'stable' configuration whereby the black hole accretes mater from an external accretion disk or just photons from the CMB. Eventually, after a gigantic span of time, the temperature falls below that of the black hole and evaporates due to Hawking radiation until it disappears (or some other unknown process takes over). Thus, after outlining briefly the formation and evolution of a black hole, we can see that the black hole is not truly static for any point in its history and therefore it is not truly Schwarzschild at any point in time. To model a realistic black hole would be an increasingly complicated problem, however this can be simplified somewhat by the Vaidya metric which assumes pressureless null dust. This is again somewhat of simplification but provide a simple way to model dynamical spacetimes, thus allowing us to generalise the LUA trajectories in black hole spacetime.

The Vaidya metric was discussed in Chapter 5 and in in-going Eddington Finkelstein coordinates it was given by Eq (5.21):

$$ds^2 = -(1 - \frac{2M(v)}{r})dv^2 + 2dvdr + r^2 d\Omega^2. \tag{7.17}$$

Where the mass function is linear in v: $M(v) = \alpha v + M_0$ where M_0 is the initial mass and $\alpha = \frac{dM}{dv}$. The linear case is used as it is the only one permitting conformal Killing horizons (9) Following the same procedure as before to find the components of acceleration:

$$a^0 = \frac{dA}{d\tau} + \frac{M}{r^2}A^2 \tag{7.18}$$

$$a^1 = \frac{dB}{d\tau} + (\frac{2M\Delta}{r^2} + \frac{dM/dv}{r})A^2 - \frac{M}{r^2} \tag{7.19}$$

$$a^2 = a^3 = 0. \tag{7.20}$$

Where $\Delta = (1 - \frac{2M(v)}{r})$. Applying the constraint found in [54], the time component is found to be:

$$\frac{da^0}{d\tau} + \frac{M}{r^2}Aa^0 - |a|^2 A = 0. \tag{7.21}$$

Similarly for the radial component: (re express fully in terms of A)

$$\frac{da^1}{d\tau} + A(\frac{rM - 2M^2 + r^2 dM/dv}{r^3}a^0 + \frac{M}{r^2}a^1) + B(\frac{M}{r^2}a^0) - |a|^2 B = 0. \tag{7.22}$$

Eq (7.21) fully re-expressed in terms of A becomes:

$$\frac{d^2A}{d\tau^2} + \frac{3M}{r^2}A\frac{dA}{d\tau} + \frac{M(r-M)}{r^4}A^3 + \frac{\dot{M}}{r^2}A^2 - (\frac{M}{r^3} + |a|^2)A = 0. \tag{7.23}$$

Where, $\dot{M} = \frac{dM}{d\tau} = \frac{dM}{dv}\frac{dv}{d\tau}$ Eq (7.23) is very similar to Eq (7.12). The only difference being an additional term taking in to account the dynamic nature of M. Taking Eq (7.23) one can again solve numerically to obtain plots of r against v.

7.4.1 Acceleration bounds in Vaidya Spacetime

One can find acceleration bounds analogous to Eq (7.13) for the LUA trajectory in Vaidya spacetime by considering the restrictions on Eq (7.23). It is of course similar to the bound found for the Schwarzschild case, with the exception of an additional term that takes into account the changing mass of the black hole region. The general bound for $\frac{dA}{d\tau}$ that applies for all points in the trajectory in Vaidya spacetime is thus:

$$\frac{dA}{d\tau} > \frac{r^2}{3M}[\frac{M}{r^3} + |a|^2 - \frac{M}{r^4}(r-M)A^2 - \frac{\dot{M}}{r^2}A]. \tag{7.24}$$

Considering the same scenario as we have in the analogous Schwarzschild scenario, where $r_{min} = 3M_0$ (M_0 is the mass of the black hole at r_{min}), we arrive at:

$$3M_0[|a|^2 - \frac{1 - 3\sqrt{3}\dot{M}}{27{M_0}^2}] < \frac{dA_0}{d\tau} < 0. \tag{7.25}$$

Rearranging and constraining $M_0 = 1$, we find again a bound on the acceleration that this time depends on $\dot{M}$, thus extending the work done by [54]:

$$|a| < (\frac{1 - 3\sqrt{3}\dot{M}}{27})^{\frac{1}{2}}. \tag{7.26}$$

7.5 4-Acceleration in Vaidya and Schwarzschild LUA trajectories

The magnitude of the four acceleration can be found via the expression:

$$|a|^2 = -\Delta(a^0)^2 + 2a^0a^1. \tag{7.27}$$

As we are considering LUA trajectories $\frac{d|a|}{d\tau} = 0$, ergo Eq (7.27) is the same at $r = r_{min}$ as other points in the trajectory. r_{min} simply refers to the distance of closest approach to the black hole region. One can therefore calculate $|a|^2$ at r_{min} where all values are known except $\frac{dA_0}{d\tau}$

Taking $x = \frac{M}{r^2}$. In Vaidya spacetime, $|a|^2$ is found to be:

$$|a|^2 = -3\Delta(\frac{dA_0}{d\tau})^2 + 2[\frac{\dot{M}}{r}(1+A_0)A_0 - x]\frac{dA_0}{d\tau} + [\frac{2\dot{M}}{r}(1+A_0)A_0 + x]xA_0^2. \tag{7.28}$$

Where A_0 is the value of A at r_{min} Thus Eq (7.28) provides a quadratic equation which can be solved trivially to provide values for $\frac{dA_0}{d\tau}$.

In Schwarzschild spacetime $\dot{M} = 0$, so Eq (7.28) becomes:

$$|a|^2 = -3\Delta(\frac{dA_0}{d\tau})^2 - 2x\frac{dA_0}{d\tau} + x^2A^2. \tag{7.29}$$

7.6 LUA Trajectories in Dirty, Dynamical Black Holes

We can further extend the calculation by considering the more generalised case of a 'dirty, dynamical black hole' in linear Vaidya spacetime. In this scenario we are modelling Rindler trajectories in black holes surrounded by a 'halo' of dark matter of mass ΔM. This cloud begins at some distance from the black hole region r_s and ends at $r_s + \Delta r_s$. Thus leaving the system with a final mass of $M(v) + \Delta M$. The mass function to model the system is given as thus:

$$M(v,r) = \begin{cases} M_0 + \alpha v & r < r_s \\ M_0 + \alpha v + \Delta M(3 - 2\frac{r-r_s}{\Delta r_s})(\frac{r-r_s}{\Delta r_s})^2 & r_s \leq r \leq r_s + \Delta r_s \\ M_0 + \alpha v + \Delta M & r_s + \Delta r_s < r. \end{cases} \tag{7.30}$$

One can set the halo to be very close to the black hole region such that $r_s = 0$, ensuring Eq (7.30) simply becomes:

$$M(v,r) = \begin{cases} M_0 + \alpha v & r \leq 2M \\ M_0 + \alpha v + \Delta M(3 - 2\frac{r}{\Delta r_s})(\frac{r}{\Delta r_s})^2 & 2M < r \leq \Delta r_s \\ M_0 + \alpha v + \Delta M & \Delta r_s < r. \end{cases} \tag{7.31}$$

The metric is thus:

$$ds^2 = -(1 - \frac{2M(v,r)}{r})dv^2 + 2dvdr + r^2d\Omega^2 \tag{7.32}$$

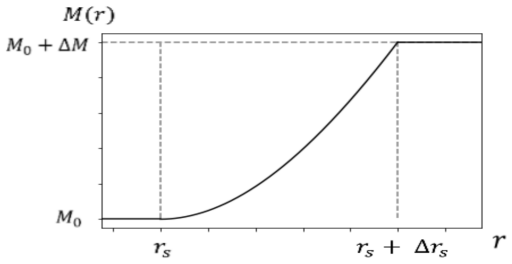

Figure 7.2: Figure of the mass function being used to model the dirty black black hole for an instant of time.

A similar time independent version of this function was used in [58] to examine the shadow of a black hole surrounded by a dark matter halo. $\Delta M > 0$ ensures a positive energy density of matter (it is also suggested that $\Delta M < 0$ can be used to analyse the behaviour of exotic, negative mass [58]). Eq (7.30) also ensures that $M(v,r)$ and dM/dr are continuous functions. The strategy is to proceed as before, whilst taking care to account for the new radial dependence of the mass. Differentiating Eq (7.31) with respect to radial position, one obtains:

$$\frac{\partial M(v,r)}{\partial r} = \begin{cases} 0 & r \leq 2M \\ 6\Delta M \frac{r}{\Delta r_s^2}(1 - \frac{r}{\Delta r_s}) & 2M < r \leq \Delta r_s \\ 0 & \Delta r_s < r. \end{cases} \tag{7.33}$$

Beginning with components of acceleration:

$$a^0 = \frac{dA}{d\tau} + (\frac{M}{r^2} - \frac{\partial M(v,r)/\partial r}{r})A^2. \tag{7.34}$$

$$a^1 = \frac{dB}{d\tau} + (\frac{M(r + 2r\frac{\partial M}{\partial r}) + r^2(\frac{\partial M}{\partial v} - \frac{\partial M}{\partial r}) - 2M^2}{r^3})A^2 - \frac{M - r\frac{\partial M}{\partial r}}{r^2}AB \tag{7.35}$$

Now one can apply the relevant constraint given by Eq (7.1), to find the time and radial components of the LUA trajectory. The time component must be of the form:

$$\frac{da^0}{d\tau} + \frac{M}{r^2}Aa^0 - |a|^2 A = 0. \tag{7.36}$$

Whilst the radial component takes the form:

$$\frac{da^1}{d\tau} + A(\frac{M(r + 2r\frac{\partial M}{\partial r}) + r^2(\frac{\partial M}{\partial v} - \frac{\partial M}{\partial r}) - 2M^2}{r^3}a^0 + \frac{M}{r^2}a^1) + B(\frac{M}{r^2}a^0) - |a|^2 B = 0. \tag{7.37}$$

Re-expressing (7.36) fully in terms of A:

$$\frac{d^2A}{d\tau^2} + \frac{3}{r}(\frac{M}{r} - \frac{\partial M}{\partial r})A\frac{dA}{d\tau} + (\frac{M(r-M)}{r^4} - \frac{3MM'}{r^3} - \frac{3M'}{2r^2})A^3 + (\frac{\dot{M}}{r^2} - \frac{\dot{M}'}{r})A^2 + (\frac{M'}{2r^2} - \frac{M}{r^3} - |a|^2)A = 0. \tag{7.38}$$

7.7 Discussion of Numerical Results

Using numerical methods and simulation, it is possible to use Eq (7.12) and Eq (7.23) to construct LUA trajectories in Schwarzschild and Vaidya spacetimes respectively and thus find Rindler horizons at some null outgoing final coordinate, u_{final}, where the LUA trajectory asymptotes to a radial outgoing null ray at $u = constant$. This section provides a discussion of the numerical results obtained, whereby Rindler horizons have been found in a dynamical background spacetime (7.7.2).

7.7.1 Numerical simulations of LUA Trajectories in Schwarzschild Spacetime

The Schwarzschild metric, as previously mentioned, provides the solution for spherically symmetric, static and stationary spacetimes, where there is no electrical charge. Therefore, describing the spacetime of a static black hole. Using Eq (7.12) and Eq (7.13) one can numerically simulate the LUA trajectories in Schwarzschild spacetime. Using the known initial values of A and B one can use Eq (7.12) to simulate the LUA trajectory, which must satisfy the acceleration bounds provided by Eq (7.13). In principle Eq (7.29) can be solved exactly for $\frac{dA_0}{d\tau}$ for given values of r_{min} and M.

In the Schwarzschild spacetime the mass of the black hole is not changing. One would expect a perturbation away from the expected LUA trajectory in the corresponding Minkowski spacetime where all initial parameters are the same. Results obtained in this thesis are akin to those obtained in [54] but in Eddington-Finkelstein coordinates.

Fig (7.3) shows the LUA trajectory starting at $r = 3M$ with $|a| = 0.1$ and $\frac{dA_0}{d\tau} = -0.3095619011$. The numerical simulation takes the trajectory out to $r = 18.5193217M$ before failing. This is perhaps most likely due to propagating error in the simulation.

Manually choosing values of $\frac{dA_0}{d\tau}$ allowed trajectories to extend further past the black hole region. Some examples are shown below. Fig (7.4) displays two plots displaying LUA trajectories in Schwarzschild spacetime with stable initial parameterisation, allowing the code to run stably. As the LUA trajectories begin at some initial r_{min} and progress radially outwards, they approaches some constant u. This is expected in Eddington-Finkelstein coordinates as lines of constant u correspond with outgoing radial null geodesics. We can also consider trajectories where r_{min} approaches $2M$, thus the LUA trajectory approaches the horizon region. One would

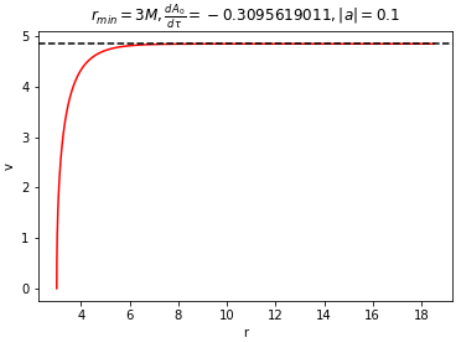

Figure 7.3: LUA trajectory in Schwarzschild spacetime for $r_{min} = 3M$, $\frac{dA_0}{d\tau} = -0.3095619011$ and $|a| = 0.1$.

expect the increasingly strong gravitational field to have some more noticeable effect on the the LUA trajectory in this case.

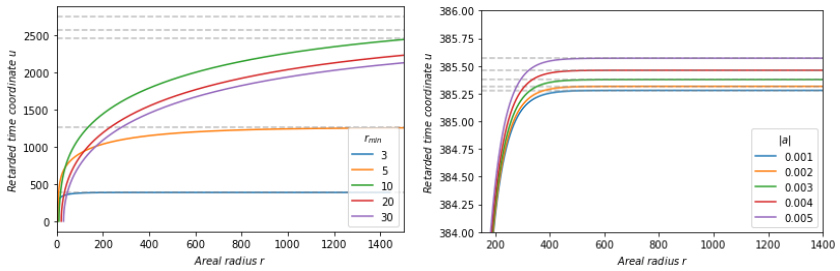

(a) (b)

Figure 7.4: (a) Five LUA trajectories for differing values of r_{min}. $|a|$ is set to 0.005, whilst $\frac{dA_0}{d\tau}$ is set to -0.00025. (b) 5 LUA trajectories this time plotted for differing values of magnitude of four-acceleration, $|a|$. r_{min} is kept at $3M$ for each trajectory whilst $\frac{dA_0}{d\tau}$ is again set to -0.00025.

r_{min}/M	u_{final}
3	385.5697643737
5	1257.130682977
10	2451.457899235
20	2563.640705689
30	2742.212107549

Table 7.1: Table showing the how the position of the Rindler horizon, u_final, changed with different r_{min} illustrated by Fig (7.4a).

Fig (7.4a) shows a plot of the equation of motion of the LUA trajectory in Schwarzschild spacetime with different values of radial distance of closest approach

$\|a\|/M$	u_{final}
0.001	385.279655845
0.002	385.315873511
0.003	385.376265392
0.004	385.460875221
0.005	385.569764373

Table 7.2: Table showing how the position of the Rindler horizon, u_{final}, changed with different values of $|a|$, illustrated by Fig (7.4b).

r_{min}. We see somewhat of a strange effect occurring in this plot, as there appears to be a non-trivial relationship between the final value of u, u_{final} and r_{min}. This relationship will be further discussed in the Vaidya case (of which Schwarzschild is a limiting case with $dM/dv = 0$). Fig (7.4b) shows a similar plot. This time the equation of motion for LUA trajectories has been plotted for different values of $|a|$ whilst r_{min} is set to $3M$ for all the trajectories. There appears to be a more straightforward relationship between $|a|$ and u_{final} with increasing $|a|$ leading to an increasing value of u_{final}. This will also be further discussed for the Vaidya spacetime.

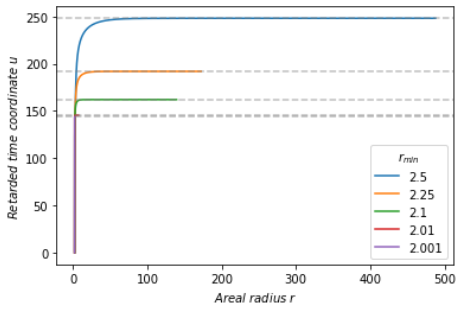

Figure 7.5: LUA trajectories in Schwarzschild spacetime for $r_{min} \to 2M$. $|a|$ is set to 0.005 and $\frac{dA_0}{d\tau} = -0.00025$.

Fig (7.5) displays plots of the equation of motion obtained numerically, when considering cases where the LUA trajectory has an r_{min} approaching $2M$. We can see that the simulation appears to reach instability much sooner than regimes with r_{min} further outside the black hole. This could be due to a higher degree of propagating error in the code when we are closer to $r = 2M$. Table (7.1) below displays how r_{final}, the final areal radius reached in the simulation before the code reaches instability, varies for different values of r_{min} in the simulation runs. These values of r_{final} are obtained from the simulation runs illustrated by Fig (7.4a) and Fig (7.5). We notice how in regimes where $r_{min} \to 2M$, the simulation appears to be quite limited for the same initial parameterisation as in Fig (7.4).

r_{min}/M	r_{final}/M
2.001	2.29238787
2.01	7.22332534
2.1	139.317547
2.25	172.254883
2.5	487.687034
3	1440.860149
5	42,908.6845
10	37,300.6617
20	169,417.717
30	48,615.0183

Table 7.3: Table showing how the final value of areal radius reached in the numerical simulation, r_{final} varies for different values of r_{min}. The values for $2.001M < r_{min} < 2.5M$ are obtained from the simulation run illustrated by Fig (7.5), whilst the values for $3M < r_{min} < 30M$ are obtained from the simulation resulting in Fig (7.4a).

7.7.2 Numerical Simulations of LUA Trajectories in linear Vaidya Spacetime

If we consider the case of a dynamical black hole spacetime where the mass parameter is a linear function of advanced time v. One can then implement a similar numerical procedure. The key difference here being the change in the black hole's mass. This procedure models a LUA trajectory away from a spherically symmetric, non-rotating black hole being irradiated by null dust. One may expect u_{final}, the final retarded time coordinate to depend on three parameters in the linear Vaidya case. Namely the radial distance of closest approach r_{min}, magnitude of 4-acceleration, $|a|$ and the rate of change of mass α. Thus we may expect u_{final} to be a three-dimensional

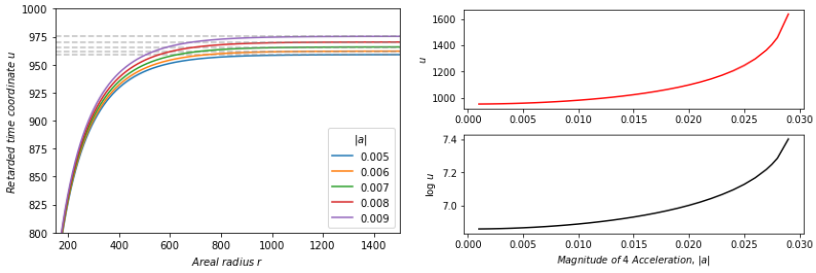

(a) (b)

Figure 7.6: (a) Five LUA trajectories in Vaidya spacetime for different values of $|a|$, with r_{min} set to $3M$ for all trajectories ,α to 0.05 and $\frac{dA_0}{d\tau} = -0.00025$. (b)Plot showing the dependence of u_{final} on $|a|$ with the corresponding log plot below.

function. We can implement a simple numerical procedure whereby we simulate the LUA trajectories, keeping two of the aforementioned variables constant whilst

changing the remaining one to analyse how u_{final} depends on the variables in question and numerically find a function that predicts the behaviour of u_{final}. In a crude sense, we shall take a one-dimensional look into the behaviour of a three-function.

$\|a\|$	u_{final}
0.005	958.96667
0.006	962.09085
0.007	965.83668
0.008	970.23315
0.009	975.31552

Table 7.4: Table showing how the position of the Rindler horizon in linear Vaidya, u_{final}, changed with different values of $|a|$, illustrated by Fig (7.6a).

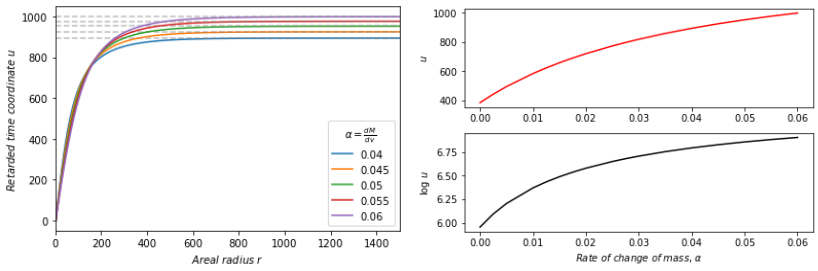

(a) (b)

Figure 7.7: (a) Five LUA trajectories in Vaidya spacetime for different values of α, with r_{min} set to $3M$ for all trajectories ,$|a|$ to 0.001 and $\frac{dA_0}{d\tau} = -0.00025$. (b)Plot showing the dependence of u_{final} on α with the corresponding log plot below.

α	u_{final}
0.04	893.93124
0.045	924.83235
0.05	952.28957
0.055	976.80684
0.06	998.79248

Table 7.5: Table showing how the position of the Rindler horizon in linear Vaidya, u_{final}, changed with different values of α, illustrated by Fig (7.7a).

Fig (7.6a), (7.7a) and (7.8a) are the main results from the simulation and display the LUA trajectory asymptoting to a Rindler horizon at constant outgoing null u coordinate. Thus forming a Rindler horizon in a dynamical background spacetime with a linear Vaidya black hole. As expected the final outgoing time coordinate u_{final} depends on three parameters, $|a|$, α and r_{min}. The dependence of u_{final} on these respective parameters is also plotted in Fig (7.6b), (7.7b) and (7.8b). We can see that Fig(7.6b) and (7.7b) appear to have a relatively straight forward functional form that appears to be

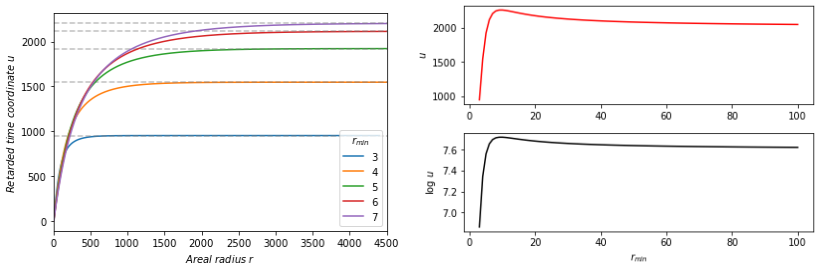

(a) (b)

Figure 7.8: (a) Five LUA trajectories in Vaidya spacetime for different values of r_{min}, with $|a|$ set to 0.001 for all trajectories ,α to 0.05 and $\frac{dA_0}{d\tau} = -0.00025$. (b)Plot showing the dependence of u_{final} on r_{min} with the corresponding log plot below.

r_{min}	u_{final}
3	952.28957
4	1547.21778
5	1922.68579
6	2115.31457
7	2205.02399

Table 7.6: Table showing how the position of the Rindler horizon in linear Vaidya, u_{final}, changed with different values of r_{min}, illustrated by Fig (7.8a).

best modelled by an exponential function and power law this can be numerically solved and fitted. However, Fig (7.8b) appears to suggest a somewhat non-trivial dependence of u_{final} on r_{min}. Where we see a peak at roughly $r = 10M$, before u_{final} begins to slowly decrease then asymptote towards the flat space solution. This effect is somewhat unexpected. One would naturally expect a more trivial dependence in this case. As r_{min} approaches the black hole we would intuitively guess that the Rindler horizons form at larger and larger u_{final}. However, results from the numerical simulation seem to indicate otherwise. This non-trivial dependence may be an opportunity for further exploration or simply refinement of the numerical method which may account for certain issues regarding the simulation. The effect of initial parameterisation via $\frac{dA_0}{d\tau}$ can not be overlooked as the simulation exhibits a great degree of sensitivity to it. Perhaps certain improvements on the numerical simulation in the future can numerically find the most suitable value of $\frac{dA_0}{d\tau}$ and provide more insight into the nature of this dependence.

Using numerical techniques, we can then find the one-dimensional functional dependence of u_{final} on the parameters in question.

Fig (7.9a) displays the simulation results for u_{final} against α the rate of change of mass of the linear Vaidya black hole. The guess function to model the simulation

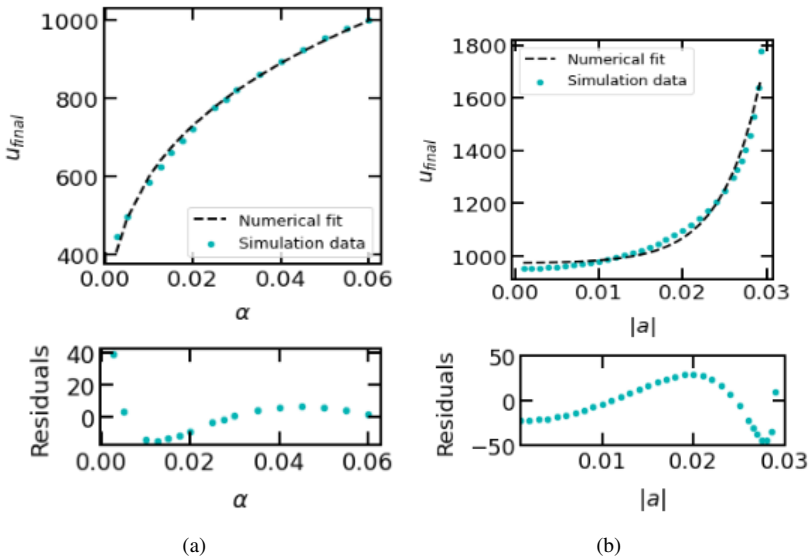

(a) (b)

Figure 7.9: (a) Simulation results for u_{final} against α with a numerical fitting and residual plot below . (b)Plot of u_{final} against $|a|$ with the corresponding residual plot below.

data was of the form $u_{final} = b\alpha^c$, where b and c are some constants. These were numerically found to be $b = 2219.37501 \pm 52.2516638$ and $c = 0.284554939 \pm 0.00657047729$. Fig (7.9b), displays simulation results for u_{final} against $|a|$, the magnitude of four-acceleration. This time the guess function was presupposed to be of the form $u_{final} = d\exp(g|a|) + h$, where d, g and h are constants. Numerically these constants were found to be: $d = 178.81195521 \pm 8.70015949$, $g = 960.28568108 \pm 6.43636961$ and $h = 3.45068686 \pm 0.85399585$. At face-value, these guess functions appear to work well numerically, with a fairly straightforward fit. However, further analysis (shown via the graph of residuals) displays an all together different story. Both Fig (7.9a) and (7.9b) display some underlying structure where higher order terms need to be taken into consideration to form a more physically accurate model of the simulation and find $u_{final}(r_{min}, |a|, \alpha)$. The non trivial dependence of u_{final} on r_{min} is perhaps also indicative of some underlying structure that is missing from our model which may rectify some errors in the simulation if it was better understood.

7.7.3 Potential Improvements and Outlook

Due to time-constraints the dirty, dynamical black hole was not simulated. Given more time, one can extend these series of simulations to account for a dynamical black hole spacetime with a radial dependence. Thus, further generalising the notion of LUA trajectories. We see no fundamental restriction to extend the code and simulation to dirty black holes. A perhaps more computationally expensive (but none the less interesting) scenario to find LUA trajectories would be in a axisymmetric head-on black

hole binary system. Binary systems have of course become of increasing interest in the Astrophysics community due to the discovery of gravitational waves from such systems [8]. We have checked the convergence of the code by reducing the step size and we find consistent results, with the trajectories asymptoting to u_{final}. In addition, we have used the code to reproduce some of the key results of [54]. With these results in hand, one can in principle relate the Unruh temperature, $T = a/2\pi$ to the surface gravity of the conformal Killing horizon at the same u value and find some thermodynamic properties relating the two.

8 CONCLUSION

The notion of an event horizon as applied to a black hole has been used for many years and has had great success, most notably in the case of the area increase law [1]. However, there are many issues that arise from the notion of event horizons leading to the unphysical properties associated with them. This is of course a problem. If black holes are truly astrophysical phenomena then this should motivate horizon notions that do away with the problems associated with event horizons. Foremost of these issues is related to the fact that event horizons are global constructs. Classically, thermodynamics is a theory based largely on localised concepts. Therefore, it appears reasonable to expect black hole thermodynamics and the related concepts that arise from it such as the entropy, Hawking radiation and surface gravity are features that can arise from quasi-local horizons. It becomes rather difficult to see how localised phenomena can depend on the event horizon. As the event horizon is highly non-local and acausal surely any physical processes that arise due to it will also be such. The non-locality of the event horizon is further highlighted in the case of a Schrodinger black hole [35]. Furthermore, the event horizon does not explicitly define the region associated with strong gravitational fields, they can arise in locally flat space. Also, one can in principle cross the event horizon without realising; their behaviour appears to be independent of local matter fluxes across them. Then we also have issues regarding how the laws of black hole dynamics were initially formulated. The zeroth law requires the notion of surface gravity which is not constructed for event horizons but for Killing horizons which coincide with event horizons only in static, stationary spacetimes. Of course, this is simply an idealisation of how the spacetime actually behaves.

Due to these considerations, it appears there is a fairly solid argument to motivate the desire to reformulate the horizon into a quasi-local concept. But this assumption might be incorrect as highlighted by Booth [34]. Black holes may just be the strangest objects in the universe which require knowledge of the entire global evolution of spacetime, thus rendering them essentially impossible for physical study. However, the theoretical developments of Hawking radiation, black hole thermodynamics and gravitational waves (which have been experimentally verified from a black hole binary system [8]), as well as theorised energy extraction processes (Penrose process) make this seem unlikely.

There are many quasi-local horizons that have been offered as alternatives to define the black hole region which we have discussed throughout this thesis and they each have their merits and drawbacks. Yet they mostly depend on the notion of marginally trapped surfaces, which intuitively capture the notion of a strong gravitational field. The Penrose singularity theorem asserts that the presence of a marginally trapped surface implies the existence of a singularity and the event horizon but not necessarily vice versa. One can also in principle find a three surface where $\theta_{(l)} = 0$ and $\theta_{(l)} < 0$ and

identify a quasi-local region that coincides with a black hole horizon [59]. Marginally trapped surfaces have also been shown to be well suited to numerical simulations where their behaviour is predictable and dependent on a stability parameter [60]. Trapping horizons which are built upon trapped surfaces have been argued as being the most suitable constructs to define the black hole region [6]. But other have suggested dynamic and isolated horizons [25] are better suited. They are essentially related and rely on trapped surfaces but have some key differences. Dynamic horizons have been shown to not enclose a trapped region[61], where as trapping horizons do. In principle, when there is a timelike trapping horizon which has a decreasing area, one can move along causal curves within the trapping horizon to the outside. This property of trapping horizons to be timelike surfaces is opposed by Ashtekar and Galloway, who argue it can not be usefully applied to the black hole surface [62].

We have also seen in the thesis the myriad of ways in which various quasi-local horizons can reproduce the zeroth, first and second laws of black hole mechanics. However, the third law remains somewhat elusive for quasi-local horizons. In fact, it has been shown that the third law may be violated in the case of non-singular black holes that permit trapping horizons [63]. In such a scenario, the inner horizon and outer horizon of a non-singular black hole meet when the final evaporation of the black hole occurs. The surface gravity then instantaneously drops to zero.

A key aspect we have not discussed in this thesis is non-uniqueness. The non-uniqueness of quasi-local horizons is a key issue in this area. For a given hypersurface, there are often more than one marginally trapped tubes, which may be endowed with a trapping horizon structure. The question naturally arises, which of these best defines the boundary of the black hole region? There appears to be no obvious way to pick. Using the entire set of dynamical horizons and marginally trapped tubes may be the answer. Krishnan discusses how each dynamical horizon obeys the dynamical horizon flux formulae [53]. But what about singular properties of the black hole, such as mass or angular momentum? Generally, different results are obtained for different choices. However, a solution to this issue has also been proposed by Bengtsson and Senovilla [64]. They propose that the 'core' of the black hole region as best suited to describe the black hole boundary. They define the core as the 'region indispensable to maintain closed trapped surfaces' and show that its boundary is the unique spherically symmetric marginally trapped tube in dynamical Vaidya spacetimes.

We have also seen in this thesis, numerical simulations of LUA trajectories that form Rindler horizons in both Schwarzschild spacetimes and in linear Vaidya spacetimes. These LUA trajectories in linear Vaidya spacetime are of special interest as we have used them to numerically find Rindler horizons in a dynamical black hole spacetime. There are some key areas of improvement and refinement with regards to the numerical simulation; notably with initial parameterisation, obtaining a greater amount of data and finding more suitable numerical fits to model the three-dimensional dependence of u_{final} on r_{min}, $|a|$ and α. None the less, we have used the numerical simulation to find Rindler horizons in a dynamical black hole spacetime, for the first time in the literature. In addition, we have derived acceleration bounds as found in [54] via alternative

considerations and extending these to the linear Vaidya case. Furthermore, we can extend the process of generalisation to dirty, dynamical spacetimes and numerically simulate the Rindler horizons in such systems. The thermodynamic properties that arise from the Rindler horizons in linear Vaidya spacetimes should also be a topic of future investigation as well as the degree to which quasi-local conformal Killing horizons inherit these thermodynamic properties.

9 APPENDIX

9.1 Finding the trapping horizon in the spherically symmetric Vaidya Metric

The spherically symmetric Vaidya line element takes the following form in advanced Eddington Finkelstein coordinates:

$$ds^2 = -\Delta(v,r)dv^2 + 2dvdr + +r^2 d\Omega^2. \tag{9.1}$$

Where $\Delta = (1 - \frac{2M(v)}{r})$. A future outer trapping horizon as defined by Hayward [48] has the following properties:

1. $\theta_l = 0$
2. $\theta_n < 0$
3. $n^a \nabla_a \theta_l < 0$.

Where l^a and n^a represent congruences of null out-going and in-going geodesics respectively. Assume l^a takes the form $(\alpha, \beta, 0, 0)$ for some arbitrary α, β such that l^a is everywhere null. One can find what form l^a takes by using the null condition: $l^a l_a = 0$:

$$l^a l_a = l^a g_{ab} l^b. \tag{9.2}$$

Where g_{ab} is the Vaidya metric in spherically symmetric spacetime. One carries out the calculation to find $l^a = \alpha(1, \frac{\Delta}{2}, 0, 0)$. If we consider this radially outgoing null vector to be parameterised by some parameter, λ, then one can deduce:

$$\frac{\Delta}{2}\frac{dv}{d\lambda} = \frac{dr}{d\lambda}. \tag{9.3}$$

Where $\alpha = \frac{dv}{d\lambda}$. Now using property 1, we require the expansion of the congruence to be 0, in order to locate a future outer trapping horizon [48]. Consider spherical isometry, such that the surface area of the congruence is simply $A = 4\pi r^2$, the expansion equation is then:

$$\begin{aligned} \theta_l &= \frac{1}{A}\frac{dA}{d\lambda} \\ &= \frac{1}{4\pi r^2}\frac{dA}{dr}\frac{dr}{d\lambda} \\ &= \frac{\Delta}{2}\frac{dv}{d\lambda}. \end{aligned} \tag{9.4}$$

One can deduce that this equals 0 at $r = 2m(v)$

This calculation can also be found and its discussion in [24].

9.2 Finding mass functions that permit conformal Killing horizons in the Vaidya metric

A metric on a pseudo-Riemannan manifold, g_{ab}^{-} is conformally related to g_{ab} via the conformal relation Eq (5.17) The conformal Killing equation is given by: $\nabla_a k_b + \nabla_b k_a = 2\Omega^2 g_{ab}$

With g_{ab} being the spherically symmetric Vaidya metric, Eq (9.1) and k^a is a spherically symmetric conformal Killing vector assumed to be of the type $(A(v,r), B(v,r), 0, 0)$. Ω^2 is the conformal factor a smooth function on our manifold.

This expression is dealing with covariant derivatives, which will require the calculation of Christoffel symbols. The Christoffel symbols required are:

$$\Gamma^v_{vv} = \frac{M(v)}{r^2} \tag{9.5}$$

$$\Gamma^r_{vv} = \frac{rM(v) - 2M(v)^2 + r^2\dot{M}(v)}{r^3} \tag{9.6}$$

$$\Gamma^r_{rv} = -\frac{M(v)}{r^2} \tag{9.7}$$

$$\Gamma^r_{\theta\theta} = -r + 2M(v). \tag{9.8}$$

Carrying out the calculation for the 'vv', 'rr' 'rv' and $\theta\theta$ equations, one finds the following expressions:

$$(-\dot{\Delta}A - \Delta\dot{A} + \dot{B} - \frac{M}{r^2}(-\Delta A + B) - \frac{rM - 2M^2 + r^2\dot{M}}{r^3}A) = -\Omega^2(1 - \frac{2M}{r}) \tag{9.9}$$

$$A' = 0 \tag{9.10}$$

$$\dot{A} + B' = 2\Omega^2 \tag{9.11}$$

$$(r - 2M)A + r(-\Delta A + B) = \Omega^2 r^2. \tag{9.12}$$

Where $\dot{A} = \frac{\partial A}{\partial v}, \dot{B} = \frac{\partial B}{\partial v}$ and similarly for $\dot{M}$. Whilst, $A' = \frac{\partial A}{\partial r}$, and $B' = \frac{\partial B}{\partial r}$. Plugging Eq (9.11) into Eq (9.9) and rearranging, one then finds a first order ordinary differential equation:

$$A\dot{M} = -\dot{B}r - B'(r - 2M) + \frac{B}{r}(r - M). \tag{9.13}$$

The Vaidya mass functions, $M(v)$, that permit conformal Killing horizons, must therefore obey Eq (9.13), which relates the mass function to the components of the conformal Killing vector.

REFERENCES

[1] J. M. Bardeen, B. Carter, and S. Hawking, "The Four laws of black hole mechanics," *Commun. Math. Phys.*, vol. 31, pp. 161–170, 1973.

[2] S. W. Hawking, "Black hole explosions," *Nature*, vol. 248, pp. 30–31, 1974.

[3] A. Strominger and C. Vafa, "Microscopic origin of the Bekenstein-Hawking entropy," *Phys. Lett. B*, vol. 379, pp. 99–104, 1996.

[4] S. W. Hawking and G. F. R. Ellis, *The large scale structure of space-time*, vol. 1. Cambridge university press, 1973.

[5] E. Curiel, "The many definitions of a black hole," *Nature Astronomy*, vol. 3, no. 1, pp. 27–34, 2019.

[6] A. B. Nielsen, "Black holes and black hole thermodynamics without event horizons," *Gen. Rel. Grav.*, vol. 41, pp. 1539–1584, 2009.

[7] R. Penrose, "Gravitational collapse and space-time singularities," *Physical Review Letters*, vol. 14, no. 3, p. 57, 1965.

[8] B. Abbott, R. Abbott, T. Abbott, M. Abernathy, F. Acernese, K. Ackley, C. Adams, T. Adams, P. Addesso, R. Adhikari, and et al., "Binary black hole mergers in the first advanced ligo observing run," *Physical Review X*, vol. 6, Oct 2016.

[9] W. G. Unruh, "Notes on black-hole evaporation," *Phys. Rev. D*, vol. 14, pp. 870–892, Aug 1976.

[10] A. C. Wall, "A proof of the generalized second law for rapidly changing fields and arbitrary horizon slices," *Phys. Rev. D*, vol. 85, p. 104049, 2012. [Erratum: Phys.Rev.D 87, 069904 (2013)].

[11] A. B. Nielsen and A. A. Shoom, "Conformal killing horizons and their thermodynamics," *Classical and Quantum Gravity*, vol. 35, no. 10, p. 105008, 2018.

[12] K. Schwarzschild, "On the gravitational field of a mass point according to Einstein's theory," *Sitzungsber. Preuss. Akad. Wiss. Berlin (Math. Phys.)*, vol. 1916, pp. 189–196, 1916.

[13] M. D. Kruskal, "Maximal extension of Schwarzschild metric," *Phys. Rev.*, vol. 119, pp. 1743–1745, 1960.

[14] G. Nordström, "On the Energy of the Gravitation field in Einstein's Theory," *Koninklijke Nederlandse Akademie van Wetenschappen Proceedings Series B Physical Sciences*, vol. 20, pp. 1238–1245, Jan. 1918.

[15] H. Reissner, "Über die eigengravitation des elektrischen feldes nach der einsteinschen theorie," *Annalen der Physik*, vol. 355, no. 9, pp. 106–120, 1916.

[16] R. Penrose, "Gravitational Collapse: the Role of General Relativity," *Nuovo Cimento Rivista Serie*, vol. 1, p. 252, Jan. 1969.

[17] D. Christodoulou, "The instability of naked singularities in the gravitational collapse of a scalar field," *Annals of Mathematics*, vol. 149, no. 1, pp. 183–217, 1999.

[18] J.-Q. Guo, L. Zhang, Y. Chen, P. S. Joshi, and H. Zhang, "Strength of the naked singularity in critical collapse," *Eur. Phys. J. C*, vol. 80, no. 10, p. 924, 2020.

[19] R. P. Kerr, "Gravitational field of a spinning mass as an example of algebraically special metrics," *Phys. Rev. Lett.*, vol. 11, pp. 237–238, Sep 1963.

[20] V. P. Frolov and A. Zelnikov, *Introduction to black hole physics*. OUP Oxford, 2011.

[21] R. Penrose and R. M. Floyd, "Extraction of rotational energy from a black hole," *Nature*, vol. 229, pp. 177–179, 1971.

[22] P. Vaidya, "The Gravitational Field of a Radiating Star," *Gen. Rel. Grav.*, vol. 31, pp. 121–135, 1999.

[23] E. Poisson, *A relativist's toolkit: the mathematics of black-hole mechanics*. Cambridge university press, 2004.

[24] A. B. Nielsen, "Revisiting vaidya horizons," *Galaxies*, vol. 2, no. 1, pp. 62–71, 2014.

[25] A. Ashtekar and B. Krishnan, "Isolated and dynamical horizons and their applications," *Living Reviews in Relativity*, vol. 7, no. 1, p. 10, 2004.

[26] D. Finkelstein, "Past-future asymmetry of the gravitational field of a point particle," *Physical Review*, vol. 110, no. 4, p. 965, 1958.

[27] S. W. Hawking, "Breakdown of predictability in gravitational collapse," *Phys. Rev. D*, vol. 14, pp. 2460–2473, Nov 1976.

[28] X. Dai, "The Black Hole Paradoxes and Possible Solutions," *J. Phys. Conf. Ser.*, vol. 1634, no. 1, p. 012088, 2020.

[29] M. J. Perry, "No future in black holes," *arXiv:2106.03715*, 2021.

[30] J. C. A. Miller-Jones *et al.*, "Cygnus X-1 contains a 21–solar mass black hole—Implications for massive star winds," *Science*, vol. 371, no. 6533, pp. 1046–1049, 2021.

[31] A. Eckart, R. Genzel, T. Ott, and F. Eisenhauer, "Stellar Proper Motions And The Dark Mass In The Galactic Center," in *32nd Rencontres de Moriond: Extragalactic Astronomy in the Infrared*, (Paris), Edition Frontieres, 1997.

[32] The Royal Swedish Academy of Sciences, "The Laser Interferometer Gravitational-Wave Observatory and the first direct observation of gravitational waves," , Oct 2017.

[33] The Royal Swedish Academy of Sciences, "The Nobel Prize in Physics 2020 Press Release," , Oct 2020.

[34] I. Booth, "Black-hole boundaries," *Canadian journal of physics*, vol. 83, no. 11, pp. 1073–1099, 2005.

[35] D. Sudarsky, "A Schroedinger black hole and its entropy," *Mod. Phys. Lett. A*, vol. 17, pp. 1047–1057, 2002.

[36] S. M. Carroll, *Spacetime and geometry*. Cambridge University Press, 2019.

[37] S. W. Hawking, "Black holes in general relativity," *Commun. Math. Phys.*, vol. 25, pp. 152–166, 1972.

[38] W. Rindler, "Hyperbolic motion in curved space time," *Phys. Rev.*, vol. 119, pp. 2082–2089, Sep 1960.

[39] B. Carter, "Properties of the Kerr metric, in Proceedings, Ecole d'Eté de Physique Théorique: Les Astres Occlus: Les Houches, France, August, 1972," vol. 23, 1973.

[40] L. Smarr, "Mass formula for Kerr black holes," *Phys. Rev. Lett.*, vol. 30, pp. 71–73, 1973. [Erratum: Phys.Rev.Lett. 30, 521–521 (1973)].

[41] A. Komar, "Covariant conservation laws in general relativity," *Phys. Rev.*, vol. 113, pp. 934–936, Feb 1959.

[42] W. Israel, "Third Law of Black-Hole Dynamics: A Formulation and Proof," *Phys. Rev. Lett.*, vol. 57, no. 4, p. 397, 1986.

[43] S. Hod, "Bekenstein's generalized second law of thermodynamics: The role of the hoop conjecture," *Phys. Lett. B*, vol. 751, pp. 241–245, 2015.

[44] W. H. Zurek, "Entropy Evaporated by a Black Hole," *Phys. Rev. Lett.*, vol. 49, pp. 1683–1686, 1982.

[45] E. Schnetter and B. Krishnan, "Nonsymmetric trapped surfaces in the schwarzschild and vaidya spacetimes," *Phys. Rev. D*, vol. 73, p. 021502, Jan 2006.

[46] M. Visser, "Gravitational vacuum polarization. i. energy conditions in the hartle-hawking vacuum," *Phys. Rev. D*, vol. 54, pp. 5103–5115, Oct 1996.

[47] C. Brans and R. H. Dicke, "Mach's principle and a relativistic theory of gravitation," *Phys. Rev.*, vol. 124, pp. 925–935, Nov 1961.

[48] S. A. Hayward, "General laws of black-hole dynamics," *Physical Review D*, vol. 49, no. 12, p. 6467, 1994.

[49] A. B. Nielsen, "Black holes without boundaries," *Int. J. Mod. Phys. D*, vol. 17, pp. 2359–2366, 2009.

[50] S. A. Hayward, *Black Holes: New Horizons*. World Scientific, 2013.

[51] A. Ashtekar, C. Beetle, and S. Fairhurst, "Mechanics of isolated horizons," *Class. Quant. Grav.*, vol. 17, pp. 253–298, 2000.

[52] A. Ashtekar, C. Beetle, and J. Lewandowski, "Geometry of generic isolated horizons," *Class. Quant. Grav.*, vol. 19, pp. 1195–1225, 2002.

[53] B. Krishnan, "Quasi-local black hole horizons," *Springer Handbook of Spacetime*, pp. 527–555, 2014.

[54] K. Paithankar and S. Kolekar, "Bound on rindler trajectories in a black hole spacetime," *Physical Review D*, vol. 99, no. 6, p. 064012, 2019.

[55] K. Paithankar and S. Kolekar, "Rindler horizons in a schwarzschild spacetime," *Physical Review D*, vol. 100, no. 8, p. 084029, 2019.

[56] A. C. Wall, "A Proof of the generalized second law for rapidly-evolving Rindler horizons," *Phys. Rev. D*, vol. 82, p. 124019, 2010.

[57] S. Kolekar and J. Louko, "Gravitational memory for uniformly accelerated observers," *Phys. Rev. D*, vol. 96, p. 024054, Jul 2017.

[58] R. A. Konoplya, "Shadow of a black hole surrounded by dark matter," *Phys. Lett. B*, vol. 795, pp. 1–6, 2019.

[59] R. Carballo-Rubio, P. Kumar, and W. Lu, "Seeking observational evidence for the formation of trapping horizons in astrophysical black holes," *Phys. Rev. D*, vol. 97, no. 12, p. 123012, 2018.

[60] D. Pook-Kolb, O. Birnholtz, B. Krishnan, and E. Schnetter, "Existence and stability of marginally trapped surfaces in black-hole spacetimes," *Phys. Rev. D*, vol. 99, no. 6, p. 064005, 2019.

[61] J. M. M. Senovilla, "On the existence of horizons in space-times with vanishing curvature invariants," *JHEP*, vol. 11, p. 046, 2003.

[62] A. Ashtekar and G. J. Galloway, "Some uniqueness results for dynamical horizons," *Adv. Theor. Math. Phys.*, vol. 9, no. 1, pp. 1–30, 2005.

[63] S. A. Hayward, "Formation and evaporation of regular black holes," *Phys. Rev. Lett.*, vol. 96, p. 031103, 2006.

[64] I. Bengtsson and J. M. M. Senovilla, "Region with trapped surfaces in spherical symmetry, its core, and their boundaries," *Phys. Rev. D*, vol. 83, p. 044012, Feb 2011.